CHALMERS
UNIVERSITY OF TECHNOLOGY

Measuring Abdominal Muscle Activity:

Design and evaluation of an electromyography prototype to enable objective diagnosis of peritonitis

Master's thesis in Biomedical Engineering

SIGNE SVENSSON
JOHANNA HENRIKSSON WENNSTRÖM

DEPARTMENT OF ELECTRICAL ENGINEERING
CHALMERS UNIVERSITY OF TECHNOLOGY
Gothenburg, Sweden 2021
www.chalmers.se

Master's thesis 2021

Measuring Abdominal Muscle Activity:

Design and evaluation of an electromyography prototype
to enable objective diagnosis of peritonitis

SIGNE SVENSSON
JOHANNA HENRIKSSON WENNSTRÖM

CHALMERS
UNIVERSITY OF TECHNOLOGY

Department of Electrical Engineering
Division of Signal Processing and Biomedical Engineering
Chalmers University of Technology
Gothenburg, Sweden 2021

Measuring Abdominal Muscle Activity:
Design and evaluation of an electromyography prototype to enable objective diagnosis of peritonitis
SIGNE SVENSSON
JOHANNA HENRIKSSON WENNSTRÖM

Supervisor: Silvia Muceli, Department of Electrical Engineering
Andreas Jonsson, Strandbacka Medical
Examiner: Sabine Reinfeldt, Department of Electrical Engineering

Master's Thesis 2021
Department of Electrical Engineering
Division of Signal Processing and Biomedical Engineering
Chalmers University of Technology
SE-412 96 Gothenburg
Telephone +46 31 772 1000

Cover: The authors at a tea party.

Typeset in LaTeX
Printed by Chalmers Reproservice
Gothenburg, Sweden 2021

Measuring Abdominal Muscle Activity:
Design and evaluation of an electromyography prototype to enable objective diagnosis of peritonitis

SIGNE SVENSSON
JOHANNA HENRIKSSON WENNSTRÖM
Department of Electrical Engineering
Chalmers University of Technology

Abstract

Peritonitis is a severe condition that currently has unreliable or time-consuming diagnosing methods. Patients suffering from peritonitis show a continuous and increased abdominal muscle activity called guarding. There is research indicating that peritonitis can be diagnosed using surface electromyography (sEMG). The purpose of this thesis was to develop a prototype that, by using sEMG, can measure small changes in abdominal muscle activity. By comparing our findings with existing research, the aim was to assess whether our prototype could be used to detect guarding and determine what future work is necessary to create a feasible product. The existing literature on the topic is very limited, but it suggests that peritonitis causes increased sEMG activity during relaxation and after coughs. Four sEMG circuits were built to enable measuring from four abdominal muscles simultaneously. Denoising and electrocardiogram (ECG) attenuating algorithms were implemented to improve the quality of the signals. Experiments were conducted on the internal and external obliques of two subjects during relaxation, voluntary tension, coughing and deep breathing. Our findings suggest that the developed prototype was successful in distinguishing small muscle activity, such as that generated by deep breathing, in all four abdominal quadrants. Further, it can detect sEMG resulting from rapid and forceful contraction, such as that generated by a cough. The combination of our findings with the findings of existing research provides some support for the conceptual idea that the created prototype can detect signs of peritonitis. However, more work, most importantly a clinical trial, is needed to verify how peritonitis manifests in sEMG signals, as well as to assess whether an sEMG device, derived from our prototype, can aid in early diagnosing of peritonitis. We believe that a clinical validation of our prototype, along with improvements in the user interface and usability, will enable the development of a final product that has potential in the medical field.

Keywords: peritonitis, surface electromyography, guarding, diagnosing, external obliques, internal obliques, prototype.

Acknowledgements

We would like to thank Andreas Jonsson for the opportunity to work with and support Strandbacka Medical in their pursuit to improve healthcare. We are very grateful for this exciting and educative experience. Moreover, we would like to thank our supervisor Silvia Muceli for her exquisite support, valuable insights, and positivity. Lastly, we want to express our gratitude towards friends and family who have supported us throughout this journey.

Signe Svensson & Johanna Henriksson Wennström, Gothenburg, June 2021

Contents

List of Figures

List of Tables

1
Introduction

Peritonitis is a severe and potentially deadly condition that currently has unreliable or time consuming diagnosing methods [1]. This thesis investigates if surface electromyography (sEMG) can be used to detect signs of peritonitis. The aim is to design and build a prototype of a device that utilizes sEMG to measure small changes in the abdominal muscle activity.

Peritonitis is an inflammation of the peritoneum [2]. The peritoneum is the largest serous membrane of the body and covers all intra-abdominal structures and the abdominal walls [3, 4]. Peritonitis is often caused by bacterial infection, but it can also be the result of fluid leakage of, for example, blood or urine [2]. It is the second leading cause of sepsis in patients in intensive care units and accounts for 1% of all emergency admissions [5]. The mortality of patients who develop sepsis from peritonitis is 35%, but the overall mortality of patients with peritonitis is approximately 6%.

Diagnosing peritonitis is traditionally done by palpation of the abdomen and estimation of the patient's pain level [1, 2]. This method is subjective and often unreliable [1, 5]. Palpation can reveal where the patient experiences most pain, as well as eventual abdominal muscle tone [6]. If a patient suffers from peritonitis, there will be a continuous tension of the abdominal muscles. This phenomenon is known as guarding [1]. Measuring the muscle activity in the abdominal muscles, and thus detect guarding, could enable a more certain and objective assessment of abdominal pain.

Surface electromyography measures muscle activity by detecting electrical potential on the surface of the skin [7]. It produces signals that contain information about muscle contraction and is widely used in rehabilitation and medical research [8]. Recent research aimed at measuring abdominal muscle activity with sEMG to detect peritonitis is very limited, despite previous research indicating that it can be done [6].

1.1 Problem Description

The objective of this thesis is to build and design a prototype of a device that utilize sEMG to measure abdominal muscle activity. The prototype should be able to detect small muscle contractions in all abdominal quadrant simultaneously. By

analyzing the measurements, it will be assessed whether this device could be used to indicate the presence of peritonitis. This assessment is done on behalf of Strandbacka Medical. Strandbacka Medical aims to create a product which can aid in objective assessment and diagnosing of peritonitis. The idea is to use sEMG to measure and detect guarding in the abdominal muscles. In contrast to diagnosing peritonitis by abdominal palpation, Strandbacka Medical aims to create a product that is quick, painless, and more accurate.

1.1.1 Aim

The aim of this master's thesis is to provide data that serves as a basis for Strandbacka Medical in the development of their product. By producing a prototype that can measure abdominal muscle activity during breathing, relaxation, tension and coughing, the project aims to draw conclusions regarding functionality and future developments of the prototype. The research questions that this thesis will answer are the following:

- Can the prototype clearly differentiate between muscle activity and relaxation?
- Does the prototype have sufficient sensitivity to detect small muscle activity, such as breathing?
- What are the characteristics of peritonitis in an sEMG recording? And would the prototype be able to detect said characteristics?
- What conclusions can be drawn regarding the product's feasibility, functionality and future developments?

1.2 Limitations

This research is limited to creating a prototype that can conduct measurements of some specific signals that may imply the presence of peritonitis. The purpose of the prototype is not to diagnose peritonitis. Further, no measurements on patients suffering from peritonitis are conducted, as this would require a clinical trial. Therefore, conclusions regarding the product feasibility are not made purely on the basis of measurements taken during this project. However, the amount of previous research available on sEMG in combination with peritonitis is very limited. The prototype is only tested on a small group of individuals, and thus, conclusions are not drawn regarding its application on a more diverse population. Measurements are only conducted on and by the thesis authors as the prototype is in an early development stage, and measurements on other subjects would require ethical approval.

1.3 Disposition

The overall structure of this study takes the form of six chapters. The thesis begins with providing a theoretical framework presented in Chapter 2. It deals with the

pathology of peritonitis and how electrical signals on the skin are generated and measured using sEMG. It also presents state-of-the-art methodology in sEMG applications. Chapter 3 is concerned with the methodology used in this study. Firstly, it provides an overview of the prototype. Secondly, the circuit properties, signal processing and hardware of the prototype is described. Thirdly, it describes how information regarding the characteristics of peritonitis in sEMG was acquired, as well as stating said characteristics. Lastly, it presents the structure and aim of the performed experiments. The fourth chapter provides the findings of the research, focusing on the signal processing, and the measurement obtained from the experiments. These results, identified limitations, and future developments are then discussed, analyzed and evaluated in Chapter 5. All findings are concluded and presented in the last chapter, Chapter 6.

2

Theory

This chapter presents the theory which provides a foundation for this master's thesis. The pathology of peritonitis and current diagnosing standards are introduced. This is followed by a general overview of muscle activity and biopotentials. Further, important technical aspects and general consensus regarding sEMG are presented. Moreover, the section covers sEMG signal properties and processing.

2.1 Peritonitis

The peritoneum is a large serous membrane that covers all intra-abdominal structures and the abdominal walls [3, 4]. The peritoneum is divided into the parietal and the visceral part. The parietal peritoneum covers the abdominal wall and the visceral peritoneum surrounds the organs in the abdominal cavity. Despite being divided into two parts, the peritoneum is one continuous membrane. Peritonitis is an inflammation of the peritoneum, which can be localized or generalized [2]. Localized peritonitis is characterized by sharp localized pain and is often associated with inflammation of the parietal peritoneum [1, 5]. Generalized peritonitis manifests as a less localized pain and is often associated with inflammation of the visceral peritoneum. Generalized peritonitis is more difficult to diagnose due to the fact that impulses from intra-abdominal organs are crudely localized. Peritonitis is often caused by bacterial infection which can be the result of, for example, acute appendicitis, colonic perforations, postoperative infections and pariteal dialysis [9, 10]. If the inflammation is not bacterial, a patient may be suffering from sterile peritonitis which can be the result of fluid leakage of, for example, blood or urine [2].

Patients with peritonitis suffer from abdominal pain, and often show signs of fever, vomiting and nausea [2, 11]. The abdominal pain can vary from mild to very intense. Depending on the severity of the inflammation, and the time from onset to treatment, the outcome varies. Peritonitis is the second leading cause of sepsis in patients in intensive care units and accounts for 1% of all emergency admissions [5]. The mortality of patients who develop sepsis from peritonitis is 35%, and the overall mortality of patients with peritonitis is approximately 6%. In addition, patients who develop sepsis are at risk of organ failure that can cause severe complications [5].

2.2 Diagnosing Peritonitis

Diagnosing peritonitis is initially done by palpation of the abdomen [1, 2]. Palpation can reveal where the patient experiences most pain, in case of localized peritonitis, as well as eventual abdominal muscle tone. During examination, the examiner applies pressure to one abdominal quadrant at a time, see Figure 2.1. Upon release, the examiner evaluates the patient's tenderness and muscle response [1]. The examiner

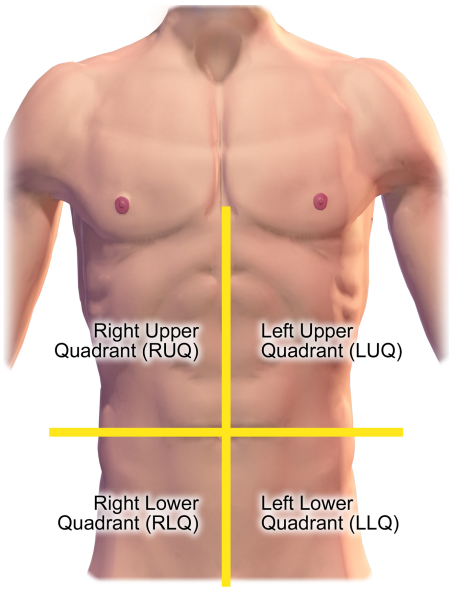

Figure 2.1: The four abdominal quadrants [12].

may also ask the patient to cough and estimate the pain response. This is known as a cough test. Moreover, the examiner evaluates the abdominal muscle activity while the patient is relaxed and breathing normally. If a patient suffers from peritonitis, there is an involuntary and continuous tension of the abdominal muscles [1, 6]. This phenomenon is known as involuntary guarding or rigidity [1, 13]. In contrast, this rigidity is not present in healthy patients. Detecting peritonitis by palpation is subjective and often unreliable [1, 5]. Consequently, laboratory tests and extensive imaging is often necessary to get a certain diagnose [5]. This exposes patients to ionizing radiation and may introduce a fatal delay before treatment [1, 5].

2.3 Muscle Activity

Skeletal muscles are the kind of muscles that can be voluntarily controlled [3]. Each muscle consists of a large number of muscle fibers [14, 15]. To initiate a contraction, an electrical signal, called an action potential, stimulates the skeletal muscle via a somatic motor neuron [3]. Each motor neuron is connected to a number of muscle fibers, and together, they are called a motor unit [14, 15]. The place where a motor neuron connects to a muscle fiber is called the neuromuscular junction. The area on a motor unit where the neuromuscular junctions are located is called the innervation zone, which is often located in the middle of a muscle [16, 17]. Since

all fibers in a motor unit are controlled by the same motor neuron, they are excited simultaneously. Upon excitation, when an action potential reaches the neuromuscular junction, acetylcholine is released. This elicits an inflow of Na^+ through the fiber membrane [3]. This inflow increases the membrane potential and gives rise to a transmembrane current that starts propagating in both directions along the membrane, causing the muscle to contract. An illustration of this process can be seen in Figure 2.2. During a muscle contraction, several motor units are activated simultaneously [3]. The intensity, or contraction force, depends on the firing rate of the action potentials, and the number of motor units activated.

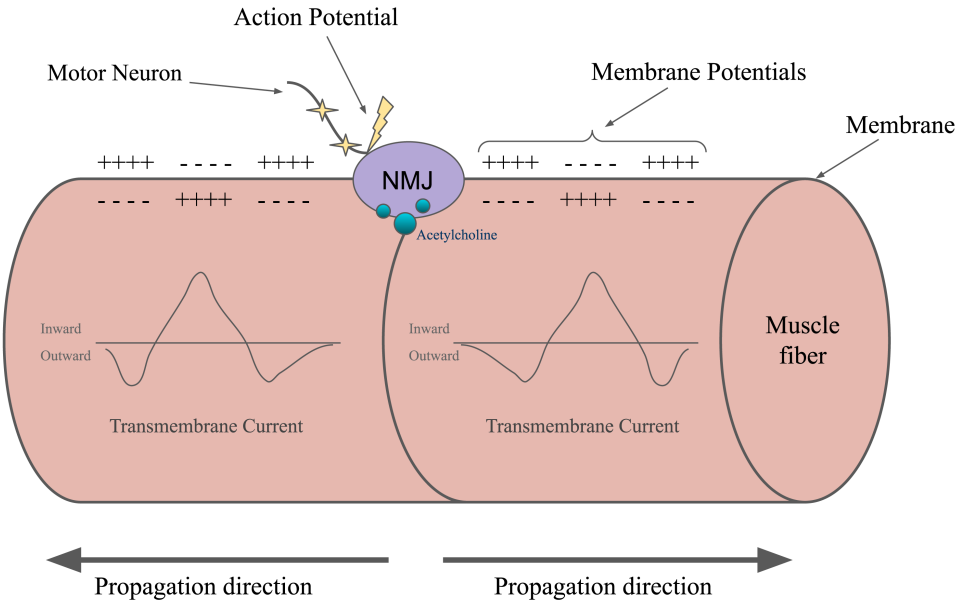

Figure 2.2: An illustration of electrical properties when an action potential reaches the neuromuscular junction, causing a contraction [3, 15, 16].

As mentioned in section 2.2, patients suffering from peritonitis may show signs of increased muscle tone and rigidness. Muscle tone is defined as the resting tension in a skeletal muscle, and it correlates to the number of motor units activated at rest [18]. Therefore, in patients with peritonitis, a high resting activity in the abdominal muscles is to be expected [6].

2.4 Surface Electromyography

Surface electromyography use non-invasive electrodes to detect electrical potential on the skin [7]. This potential is a summation of action potentials generated during muscle contraction [19]. Hence, a more forceful contraction results in a higher electrical potential on the skin. The amplitude of an sEMG signal during voluntary contraction is in the range of 0.1μV-2mV, and depends on muscle and contraction strength [20]. With increasing distance between the muscle of interest and the surface of the skin, sEMG amplitude decreases while the interference from neighbouring

muscles increases [16]. Therefore, sEMG is only applied on superficial muscles.

2.4.1 Electrode Configurations

There are a variety of configurations used to conduct sEMG measurements [16]. The most suitable one depends on the muscle and the properties of interest. The most common configurations are monopolar (MP), single differential (SD), and double differential (DD), illustrated in Figure 2.3 [20]. MP detection measures potential with respect to a reference electrode placed on an electrically inactive region [16]. This configuration can measure potential generated by sources far away. However, it is sensitive to noise and common mode signals, which is caused by for example power line interference and other muscles [20]. Therefore, MP detection is mainly used in research applications. SD detection measures the difference between two close points by comparing the potentials of two adjacent electrodes [16]. The two points are recommended to be aligned with the direction of the muscle fibers, and on the same side with respect to the innervation zone. By taking the voltage difference between two points, SD configurations cancels out common mode signals [21]. Compared to MP detection, SD detection is less sensitive to noise, but it can only detect superficial and near sources. SD detection is the most used type of modality. DD configurations further reduces common mode signals and is often used to estimate the propagation velocity of a motor unit action potential [16].

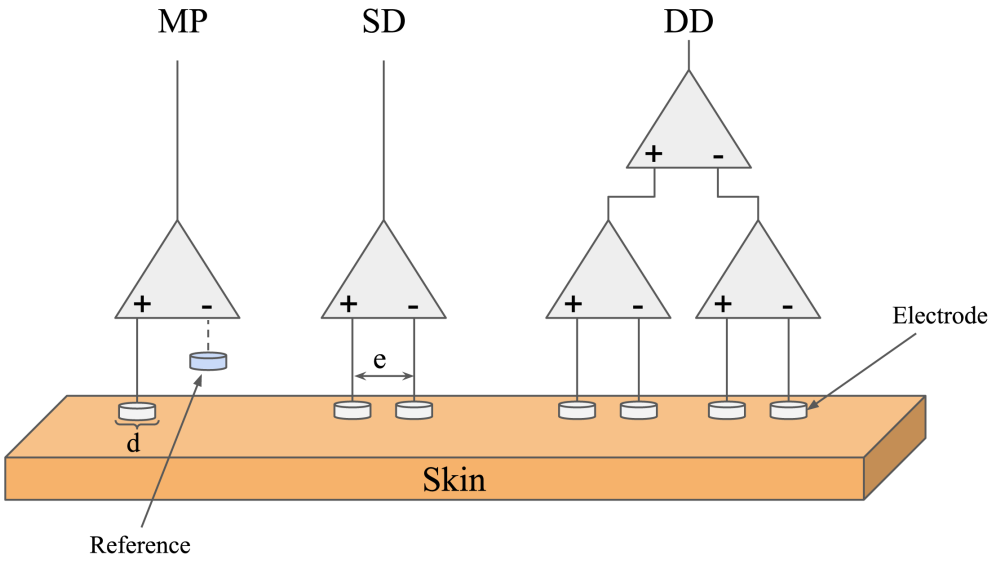

Figure 2.3: Illustration of three different electrode configurations; monopolar (MP), single differential (SD) and double differential (DD) [16].

2.4.2 Inter Electrode Distance

The quality of sEMG signals greatly depends on the inter electrode distance (IED) [20]. The IED, marked with 'e' in Figure 2.3 and Figure 2.4, is the distance between two bipolar electrodes. Recommendations for sensor placements and procedures has

been developed by the European Union through the surface electromyography for the non-invasive assessment of muscles (SENIAM) project [22]. According to the SENIAM project, the IED should not exceed 20mm. In case of measurements on small muscles, the IED should not exceed 1/4 of the total muscle fibre length. These recommendations are approximately two decades old, and more recent studies show that an IED over 10mm can distort the sEMG [16, 23]. This distortion is due to a spatial filter introduced by the SD configuration. The properties of this spatial filter depends on the IED [24, 25].

An sEMG signal is the sum of many harmonics, or frequency components, with different wavelengths, λ [16]. These wavelengths depend on their conduction velocity v and period T, see Equation 2.1. When the IED, e, is a scalar multiple of λ, the voltage measured at each bipolar electrode will be equal, see Equation 2.2. Consequently, the differential voltage will be zero, as illustrated in Figure 2.4.

$$\lambda = v \cdot T \tag{2.1}$$

$$e = \lambda \cdot n \quad \text{where } n = 1, 2, 3, ... \tag{2.2}$$

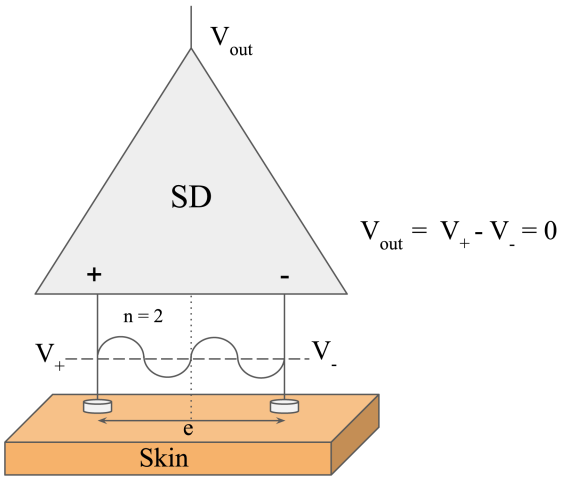

Figure 2.4: Illustration of harmonic cancellation. The inter electrode distance is e and the scalar multiple is n=2. The voltage difference between the two electrodes is zero.

This means that the spatial filter introduced by the SD configuration is a band-pass filter, see Figure 2.5. With a decrease in IED, the central frequency and bandwidth of the filter will increase [24]. In addition, cross-talk, which is defined as the interfering signals from other muscles, is also decreased with smaller IED [26]. Hence, a low IED is desirable [16]. Nevertheless, despite a low IED, high frequency components will still be attenuated [24]. This is due to low-pass filtering caused by muscle, fat and skin tissue. Consequently, even if the IED and its spatial filtering is considered, some attenuation of the high frequency components of the sEMG signal is to be expected.

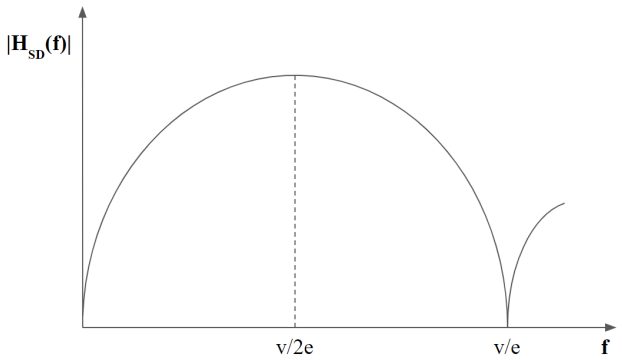

Figure 2.5: The spatial filtering introduced with bipolar electrodes in a single differential configuration [23].

2.4.3 Electrode Size

According to SENIAM, electrode size is defined as the size of the conductive area on the surface of an electrode [22]. The most common electrode shape is circular and the electrode size is presented as the diameter of the electrode [21]. Electrode size greatly affects the spectral properties of the sEMG signal [20]. Much like the IED, with an increased electrode diameter, high frequency components are attenuated [20, 24]. The conductive area of the electrode averages the voltage distribution under it. This generates a smoothed version of the actual spatial potential distribution. Consequently, the electrode creates a low-pass filter whose cut-off frequency decreases with an increased surface area [16, 20]. However, a smaller surface comes at the expense of increased skin surface impedance, and thus, noise [24]. Considering this trade-off, the recommended electrode size is in the range of 1-5mm [16, 20]. However, for non-critical applications, a bigger electrode size is acceptable [16].

2.4.4 Electrode Placement

The sEMG signal quality is affected by electrode position in regards to muscle fiber orientation and innervation zone [20, 27]. To acquire optimal sEMG measurements, electrodes should be placed in parallel to the muscle fiber direction [21, 27]. Furthermore, it is of great importance how the electrodes are placed in regards to the innervation zone. If two electrodes are placed on each side of, and equally far from a neuromuscular junction, the differential signal will be theoretically zero, as illustrated in Figure 2.6. Action potentials propagate out from the neuromuscular junction in both directions, hence, the potential will be equal on both sides [16]. In practice, this differential signal is not zero since neuromuscular junctions are distributed over the entire innervation zone. Moreover, placing surface electrodes over an innervation zone will greatly influence the signal amplitude [28, 29]. Because of this, it is well established that electrodes should not be placed over innervation zones. This is extra important when the relationship between signal amplitude and muscle activation level is of interest [30]. In addition, electrodes should not be placed close to tendons [31]. When an action potential reaches a tendon, its electrical properties changes significantly and non-propagating components occur [7, 16]. This so called

end-fiber effect can strongly influence the surface potential, even on the skin above neighbouring muscles. Therefore, placing electrodes close to tendons increases cross-talk and may cause distortion of the signal [7, 16]. For these reasons, the general consensus is that electrodes should be placed in parallel to muscle fibers and between the innervation zone and muscle tendon.

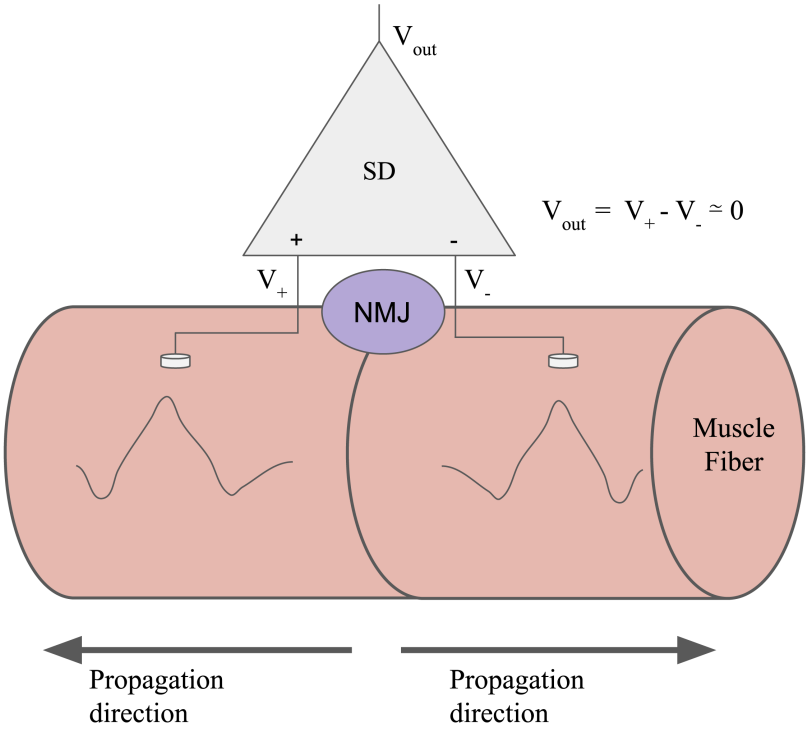

Figure 2.6: Illustration of the differential sEMG signal when electrodes are placed symmetrically over a neuromuscular junction.

To acquire accurate and stable measurements it is important that the electrode-skin impedance is low [20]. Generally, electrode-to-skin noise is the key source of noise in sEMG applications, and consequently, electrode material and skin preparation must be considered [31]. Most applications use Ag/AgCl electrodes since they provide low noise, low electrode-skin impedance and are greatly available [32]. They are often combined with conductive gel between the electrode and skin to further reduce impedance and noise. Noise can also be reduced by skin preparation [31]. This preparation usually consists of rubbing the skin with an abrasive paste to remove dead cells, and thus, minimize the thickness of the skin [20]. Taking these measures can significantly improve the quality of sEMG signals.

2.4.5 Instrumentation

The potentials of sEMG signals are in the range of 0.1μV-2mV, and hence, require amplification [20]. In a SD configuration, a front-end amplifier in the form of a differential amplifier is often and preferably used [16]. A differential amplifier is required to have high input impedance, high common mode rejection ratio (CMRR)

and low noise [20, 31]. Input impedance above 100MΩ is considered acceptable, however, higher is preferable [20]. CMRR is defined as the ratio between differential and common mode signal amplitude, A_{dm}/A_{cm}, and an acceptable value is ∼100dB [16, 31]. To avoid saturation, a front-end amplifier should only apply a moderate amount of gain [31]. To achieve a sufficient total gain, which results in the signal having a maximum peak-to-peak amplitude that fits the input range of the A/D converter, an additional amplifier can be added after filtering. The input range of an A/D converter is often around ±5V, and thus, a total gain of ∼1000 is often used, but this depends on the expected sEMG signal amplitude [31].

To achieve useful measurements, the sEMG signal must be processed to remove unwanted frequencies and noise. In general, the highest muscle harmonic of relevance is in the range of 400-450Hz [31]. Therefore, it is common to low-pass filter sEMG signals with a cut-off frequency in this range [8, 20, 28, 31, 33, 34]. To avoid aliasing, according to the Nyquist sampling theorem seen in Equation 2.3, the minimum sampling frequency, f_s, must be greater than twice the maximum frequency, f_{max} [20]. This means, that in general, the minimum sampling frequency is approximately 1000Hz for most sEMG applications. However, in many cases, the sampling frequency is 2048Hz due to technical advantages [8, 20, 28, 31, 33, 34].

$$f_s > f_{max} \cdot 2 \tag{2.3}$$

Noise that is due to, for example, motion artifacts and electrode sliding, is in the low frequency range [31]. Generally, a high-pass filter is applied to cancel that noise. The cut-off frequency of this filter is often in the range of 10-20Hz [8, 20, 28, 31, 33, 34]. Both low and high-pass filters are recommended to be of second order or more [20]. A common type of noise that affects sEMG is power line interference (PLI) [20]. It has its fundamental frequency in the 50Hz region, and is caused by power supply lines that support the sEMG device itself, or other surrounding devices [32]. It also generates noise in 50Hz harmonics, which are due to connected non-linear loads [35]. Power lines introduce electric and magnetic fields that couple onto the patient and/or the sEMG wires, and thus, cause disturbances. There are several approaches to reduce PLI, such as notch filters, spectral interpolation, and driven-right-leg (DRL) circuits [20]. DRL circuits are often used since they cancel PLI without attenuating the biopotential signal [36]. They do so by inverting and amplifying the common mode voltage on the body and feeding it back via a reference electrode [32]. This results in a reduced common mode voltage.

2.5 Wavelet Filtering

Wavelets are a powerful mathematical tool that can be used for data denoising [37]. Studies show that by applying the wavelet transform and analyzing the signal decomposition, features from sEMG signals, such as the electrocardiogram (ECG), can be extracted [38–40]. In contrast to the windowed Fourier transform, the wavelet transform uses an adaptive time-frequency resolution [37, 41]. This means that the wavelet transform contains information about where frequency components are

located in time, and maintains an adequate resolution for all details. A wavelet decomposition consists of approximation coefficients and detail coefficients [37, 41]. The approximation coefficients are generated by low-pass filtering and down-sampling the signal by removing every other data point. The detail coefficients are produced by high-pass filtering and down-sampling accordingly. The shape of the high- and low-pass filters depend on which wavelet is used in the transform. There are many different wavelets and which one is optimal depends on the application and required resolution [41]. To remove or extract ECG, it has been shown that the Daubechies 4 wavelet is suitable [38, 39]. As their names hints, the detail coefficients contain detailed information about the signal whilst the approximation coefficients contains coarse signal information [37, 41]. This process is iterated, creating several decomposition levels. The approximation details of the previous level is low- and high-pass filtered to create the decomposition of the new level, as seen in Figure 2.7. Consequently, the signal is decomposed into several levels, with each level containing more coarse features. To reconstruct the signal, the levels are up-sampled and filtered, using a filter that is similar to the decomposition filter [37].

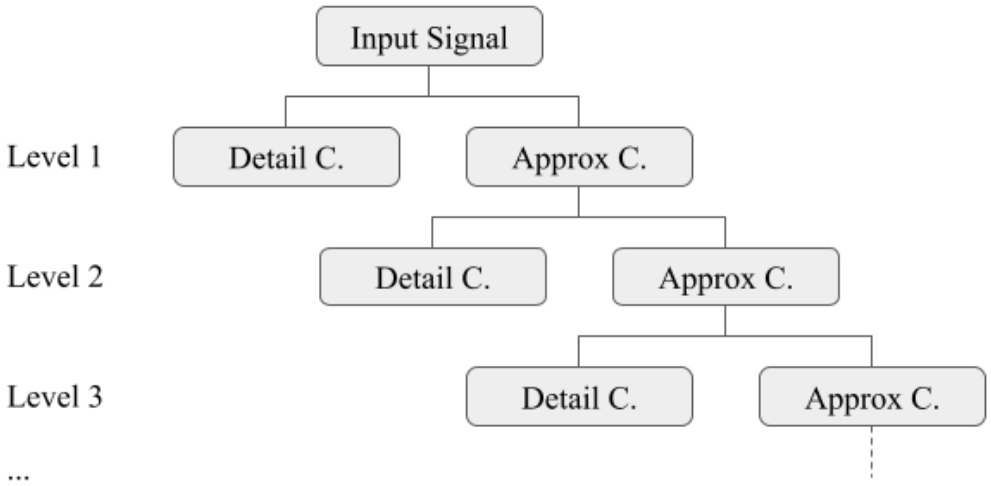

Figure 2.7: Illustration of the wavelet decomposition process. For each level, the detail coefficients describe coarser frequency components of the input signal.

2.6 Peritonitis in sEMG Recordings

There exists one study regarding how guarding looks like in sEMG recordings. This study was conducted by Rozin and Meyer in 1973 [6]. By measuring electrical activity on the internal and external obliques using sEMG, they managed to diagnose 35 out of 38 patients suffering from peritonitis. In addition, this method did not generate any false positives. The study found that there are electrical differences between healthy patients and patients with peritonitis, as presented in Table 2.1. During rest, patients suffering from peritonitis had an increased electrical activity of $\sim$ 22% of a voluntary contraction, compared to healthy subjects. In addition,

patients with peritonitis showed residual electrical activity after cough tests and palpation, which is not present in healthy individuals. It is not presented on which muscle or abdominal quadrant these characteristics were measured.

Table 2.1: sEMG characteristics for patients with and without peritonitis, according to [6].

State	**No peritonitis**	**Peritonitis**
Rest	Electrical silence	Raised electrical activity $V_{max} = 430$uV
Voluntary contraction	Electrical activity of ∼1mV	-
Cough	No residual activity	Residual electrical activity 200ms after the cough
Contralateral pressure	No residual activity	High voltage burst followed by electrical activity for 250ms after pressure

3
Methods

This chapter presents the methodology used to create the sEMG amplifier prototype, as well as the conducted experiments to evaluate its performance. Initially, a circuit was designed in accordance to the information presented in section 2.4. After realization, using the materials described in this section, software to process and display the measurements was created. To evaluate the prototype's performance, several experiments were conducted. This chapter will explain each of these steps in detail.

3.1 Prototype Overview

As described in section 2.1, patients suffering from peritonitis have an increased abdominal muscle activity. The prototype measures muscle activity in all four abdominal quadrants simultaneously. It does so by using four bipolar electrode pairs that are placed in one quadrant each. All pairs share one reference electrode, which is placed on top of the left hand. The placements can be seen in Figure 3.1, which were in accordance to the recommendations by Ng. et al [27]. The electrodes were positioned on the exterior and interior oblique muscles on both the left and right side of the abdomen. The oblique muscles were chosen since they are superficial muscles that are located in one abdominal quadrant each [3]. All electrode pairs were placed along the muscle fibers directions and connected to the prototype via 3.5mm jack outlets. The output signals are connected to a NI ELVIS II+ platform which serves as an A/D converter. The digital signals are then processed and displayed using MatLab.

3.2 Properties & Design

The prototype consists of four identical sEMG circuits, one for each electrode pair. Each sEMG amplifier circuit consists of various hardware components. Firstly, there are the electrodes and cables, followed by a differential amplifier, low-pass filter, high-pass filter and an A/D converter. The specified properties of the sEMG hardware are shown in Figure 3.2. To obtain sEMG measurements, pre-gelled Ag/AgCl electrodes in a single differential configuration was used. The electrodes had a sensor area of 15.8mm^2 and gel area of 254mm^2, which corresponds to a measuring area with a diameter of approximately 18mm. Noticeably, this is higher than the preferred conductive sensor area [16]. Electrodes that have a conductive area with a diameter smaller than 10mm, as discussed in subsection 2.4.3, was hard to come

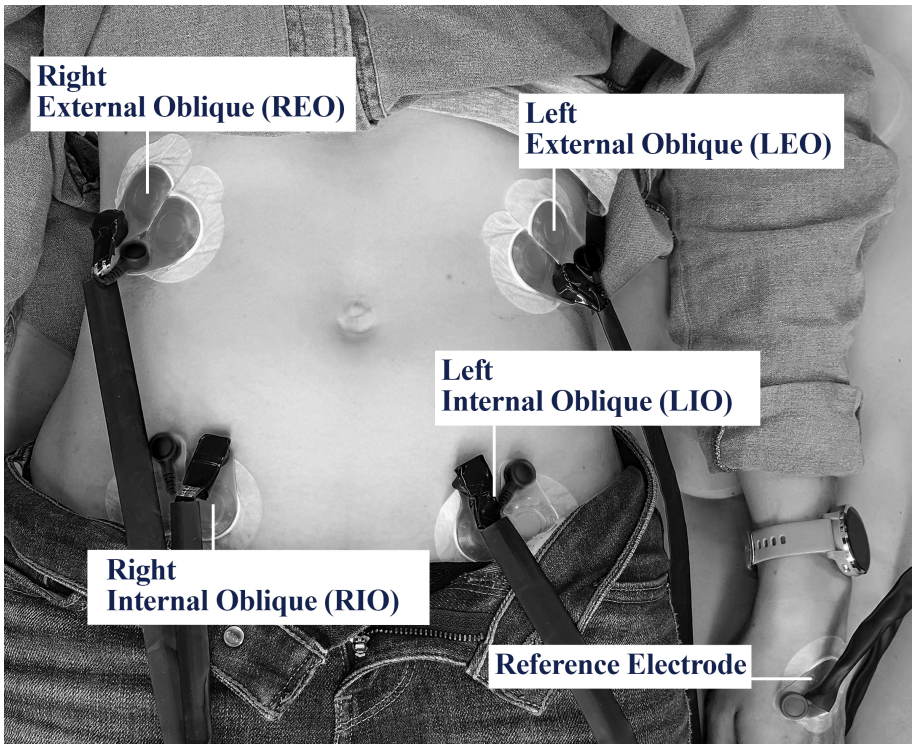

Figure 3.1: Electrode placements. The placements are in accordance to the recommendations by Ng. et al. when measuring the activity of the exterior and interior oblique muscles [27].

Sensor	Differential Amplifier	High Pass Filter	Low Pass Filter	Amplification stage	A/D Conv
Pre-gelled Ag/AgCl	Instrumentation amplifier	Cut-off: 15.76 Hz	Cut-off: 450.8 Hz	Gain: 101	Sampling frequency: 2048 Hz
SD configuration	CMRR: 110 dB	2nd order Sallen-Key	2nd order Sallen-Key		Number of bits: 16
Sensor area: 15.8 mm^2 Gel area: 254 mm^2	High input impedance	Q-factor: 0.707	Q-factor: 0.707		Input Range: ±5 V
Inter electrode distance: 21 mm	Gain: 100	Gain: 1	Gain: 1		

Figure 3.2: Properties of the prototype's hardware circuit.

by. This was due to a limited budget and limited amount of suppliers in Sweden. However, it was determined that bigger electrodes could be used since the spectral filtering they introduce is acceptable in these initial tests and application. In future

experiments and iterations of the prototype, smaller electrodes are preferable. The electrodes were spaced apart with an IED of 21mm. This was the smallest distance possible with the chosen electrodes. As discussed in subsection 2.4.2, an IED bigger than 10mm can distort the sEMG signal due to spatial filtering. In addition, it increases the risk of cross-talk. This is something that has to be taken into consideration when analyzing the results.

The differential amplifiers used in the prototype is the AD621 instrumentation amplifier from Analog Devices. This type of amplifier has high input impedance and a CMRR of 110dB. The amplifier also outputs the common mode voltage. This is used to create a driven-right-leg (DRL) system that uses the reference electrode to feedback the inverted common mode voltage, which reduces PLI [32]. As all electrode pairs share the reference electrode, this feedback is only done in one of the four sEMG circuits. Due to the low signal amplitudes generated by abdominal muscles, a gain of 100 was chosen in this step.

The analog high- and low-pass filters were designed as second order Sallen-Key filters. This was due to their simplicity and since studies show that second order filters are sufficient in sEMG hardware [8, 20]. A filter's Q-factor affects the shape of its frequency response, as seen in Figure 3.3. To achieve as constant gain as possible, the Q-factor of both filters was set to 0.707. As motivated in subsection 2.4.5, the cut-off frequencies of the high- and low-pass filters were set to 15.76Hz and 450.8Hz respectively.

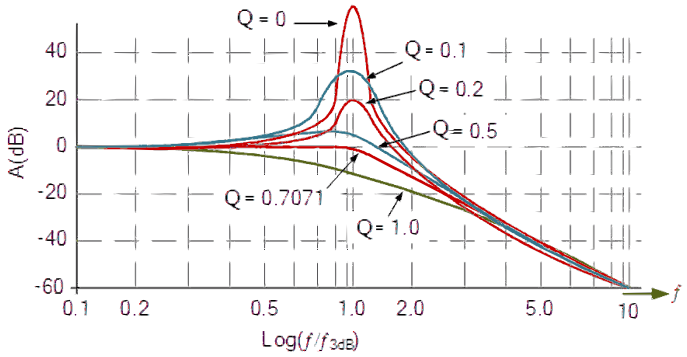

Figure 3.3: The effect different Q-factors have on filter frequency response.

In the amplification stage the gain was set to 101, which results in a total gain of 10100. As discussed in subsection 2.4.5, the gain of sEMG devices is usually around 1000. However, the muscles that are measured in this application generate weak signals. To match the input range of the A/D converter, $\pm 5V$, a higher gain was chosen. The sampling frequency was 2048Hz. Since the cut-off frequency of the low-pass filter is 450.8Hz, aliasing was avoided. The number of bits in the A/D converter was 16, which provides an input resolution of 0.152mV, as seen in Equation 3.1.

$$\frac{10}{2^{16}-1} = 0.152mV \tag{3.1}$$

3.2.1 Electrical Circuit

To achieve the properties and parameters described in section 3.2, four circuits were soldered in accordance to Figure 3.4. However, as described previously, only one of the circuits included the DRL-system, which is connected to the first of the four sEMG circuits. The supply voltage, V_s, is provided using two 9V batteries which results in a range of $\pm 9V$. The second supply voltage, V_{s2}, is provided by the NI ELVIS II+ platform and it supplies the isolation stage with $\pm 15V$. By isolating the circuit from devices powered by the power grid, the circuit, as well as the subject, is protected [32].

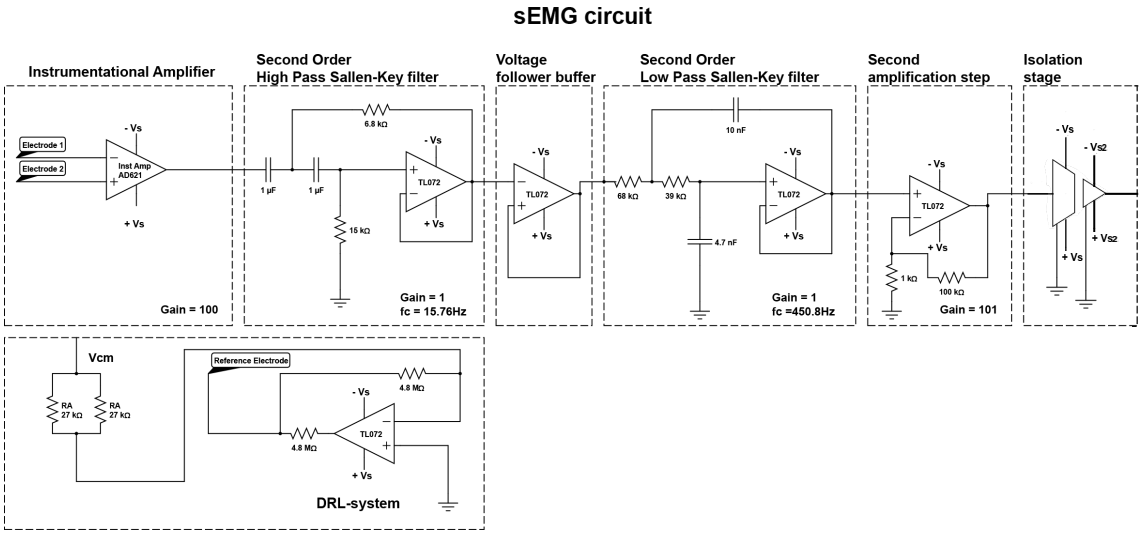

Figure 3.4: The prototype's circuit design. The bottom part containing the driven-right-leg (DRL) system is only implemented in one of the four circuits since only one reference electrode is used.

The sEMG circuits were realized using the components presented in Table 3.1. The complete circuit can be seen in Figure 3.5.

Table 3.1: Component list. Components used to realize the circuit.

Component	**Quantity**	**Manufacturer**	**Name**
9V Batteries	2	Energizer	9V Industrial
Electrodes	9	AMBU	BLUE L-00-S
Electrode cables	5	Plastics One Inc	SNAP 222
Instrumentation Amplifier	4	Analog Devices	AD621
Operational Amplifier	9	Texas Instruments	TL072CP
Isolation Amplifier	4	Texas Instruments	ISO122
A/D Converter	1	National Instruments	NI ELVIS II+
Solder board	1	Scankemi Sweden	FR4 3-track chains

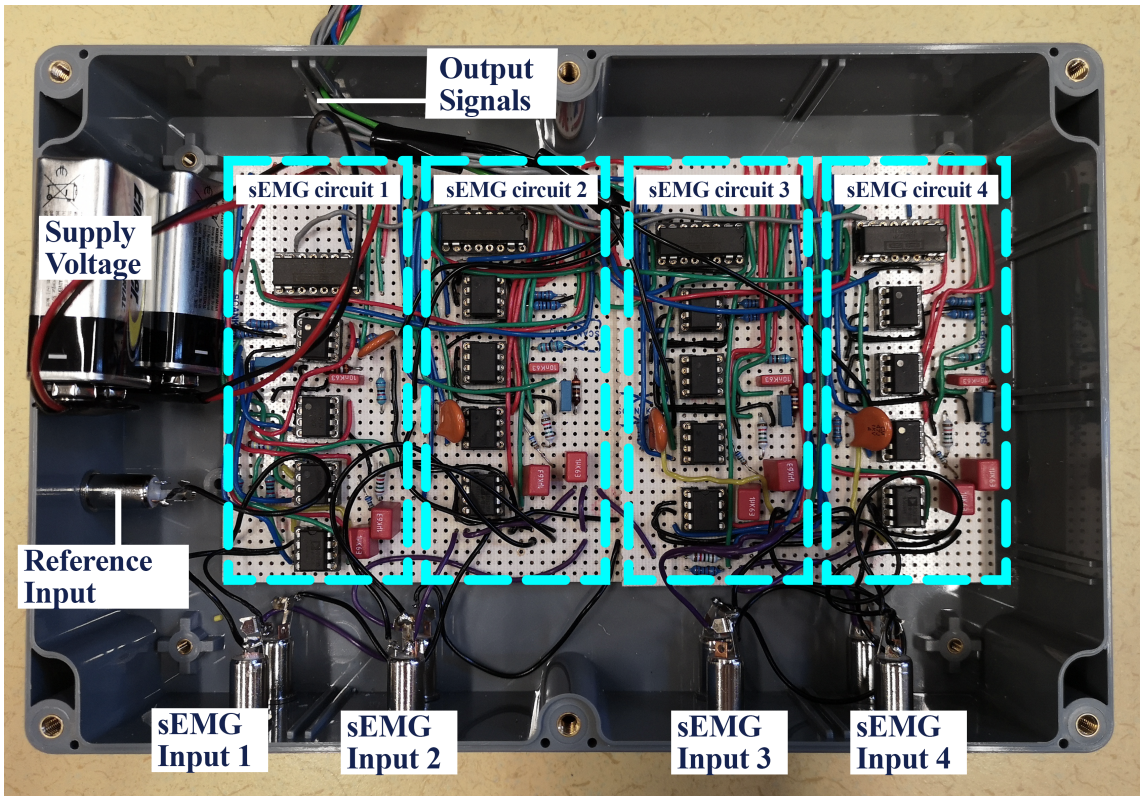

Figure 3.5: Finished circuit. The total circuit consists of four identical sEMG circuits, one for each abdominal quadrant. The driven-right-leg system is incorporated into sEMG circuit one.

3.3 Software & Signal Processing

To collect, process, and analyse the digital signals, MatLab was used. To improve the signal quality and reduce noise, digital filters were implemented. A second order band-pass filter with the same cut-off frequencies as the analog filters were used to remove additional unwanted frequency components. To remove PLI, notch filters centered around 50Hz, and its harmonics of 100Hz, 150Hz, 200Hz, 250Hz, 300Hz and 350Hz were used. As discussed by [20], notch filters change the waveform of the sEMG signal. However, in these measurements, the signal alteration introduced by the notch filters were deemed acceptable. In this application, the property of interest is muscle activation and relaxation, not the specific shape of the signal.

During the initial tests, it was observed that ECG artifacts were affecting the sEMG signals. Wavelets, namely the daubechies 4 (DB4) wavelet, was utilized to remove the ECG noise. The DB4 wavelet has a similar shape to an ECG curve, and therefore, it is preferred when aiming to detect ECG curves within a signal [38, 39]. Upon investigation, it was determined that most of the ECG artifacts were present in level 4, 5, 6 and 7 of the wavelet decomposition. This is evident in Figure 3.6, which shows a decomposition of an exterior oblique muscle signal during relaxation.

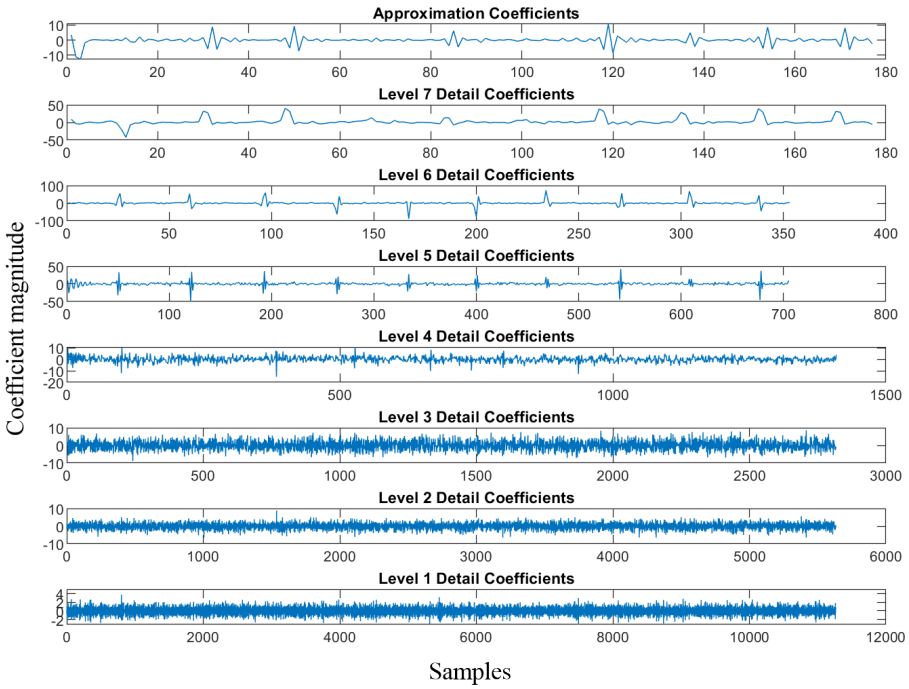

Figure 3.6: Wavelet decomposition of a signal recorded on the exterior oblique muscle during rest. There are ECG artifacts present in the decomposition levels 4, 5, 6, and 7.

To attenuate ECG artifacts without compromising the signal quality, three approaches were considered:

1. Zeroing all level 5 detail coefficients.
   - Benefits: Efficiently cancels ECG artifacts.
   - Drawbacks: Attenuates bandwidth containing much of the muscle signal.
2. Zeroing all level 7 and level 6 detail coefficients.
   - Benefits: Attenuates ECG without compromising the signal amplitude significantly.
   - Drawbacks: Does not completely remove ECG artifacts.
3. Threshold detail coefficients of level 4, 5, 6 and 7.
   - Benefits: Attenuates ECG without compromising the signal amplitude.
   - Drawbacks: Does not identify all ECG artifacts if the thresholding limit is poor.

The plot illustrating the effects of approach 1, namely zeroing all detail coefficients in level 5 of the wavelet decomposition, is presented in Figure 3.7. The figure displays the average rectified value of the signals, which is a common way of plotting a signal envelope. The rectified signals have been averaged with a 200 samples wide window, which corresponds to a time window of approximately 97.6ms. The signal depicted in Figure 3.7 is of an exterior oblique muscle contracting in intervals. As can be seen, a lot of the low frequency components are attenuated, which consequently compromises the amplitude of the signal.

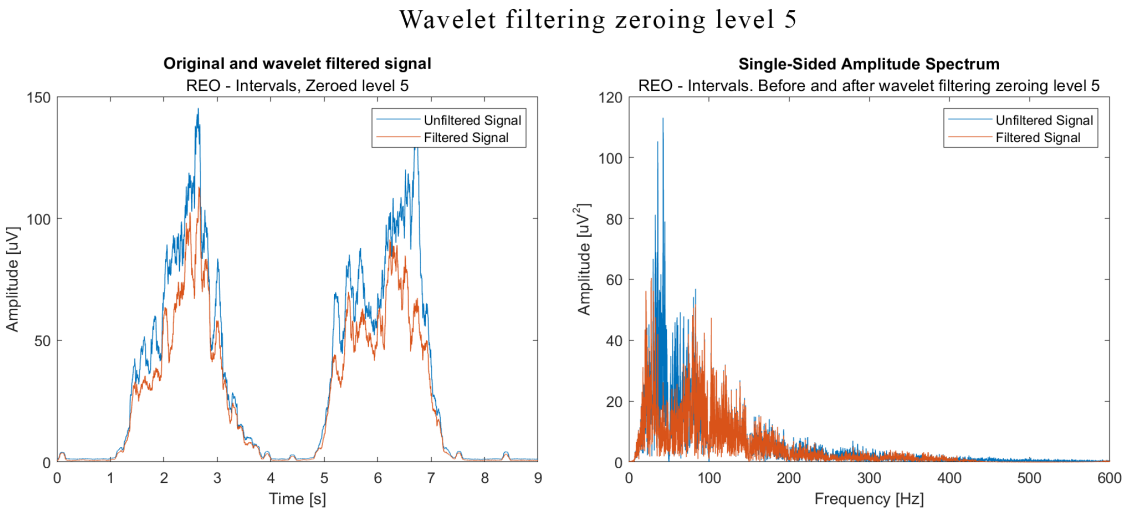

Figure 3.7: Effects of wavelet filtering when zeroing all level 5 detail coefficients. The amplitude of the time domain signal is compromised, but ECG artifacts are slightly attenuated. The frequency spectrum is heavily affected. The measurement is of a right exterior oblique (REO) muscle.

The effects of approach 2, which zeroes all detail coefficients in level 6 and 7 of the wavelet decomposition, is presented in Figure 3.8. Here, less of the muscle activity is attenuated, but the ECG artifacts are not completely eliminated.

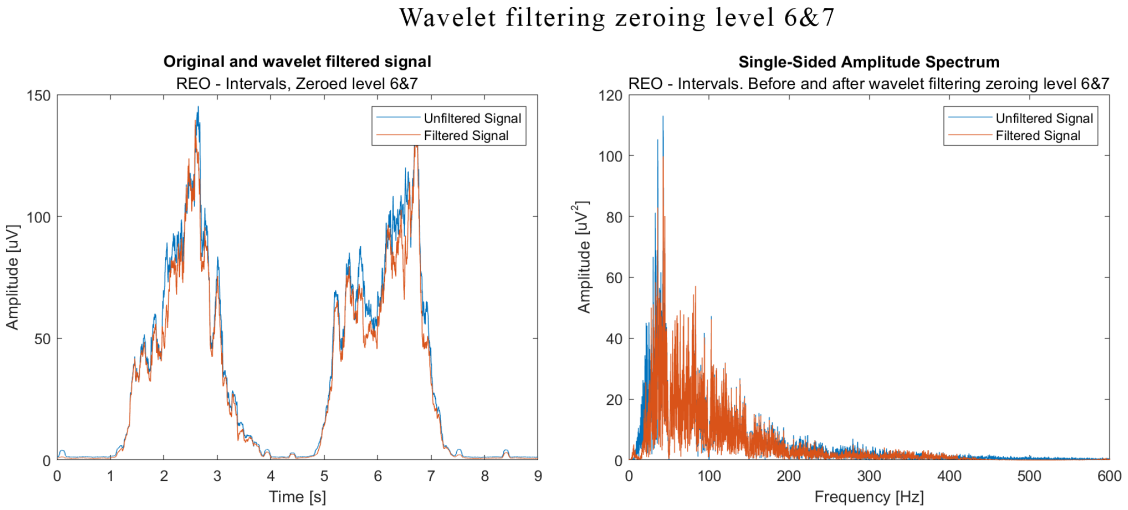

Figure 3.8: Effects of wavelet filtering when zeroing all level 6 and 7 detail coefficients. The signal in the time domain is slightly affected and the ECG artifacts are marginally attenuated. Low frequency components are compromised. The measurement is of a right exterior oblique (REO) muscle.

Approach 3 uses thresholding to cancel out the relevant detail coefficients of level 4, 5, 6, and 7. This is done by using a signal recorded during rest (no muscle activity) as reference since it contains only ECG artifacts. The reference signal is decom-

posed, as seen in Figure 3.6, and the maximum amplitude in each level, which stems from the ECG peaks, is used to determine the thresholds. This means that level 4, 5, 6 and 7 all have their individual threshold. To ensure that the thresholding is satisfactory, meaning that all ECG artifacts are found and attenuated, the threshold is set to 10% above the maximum amplitude of the reference decomposition. All detail coefficients, which are below its specific level's threshold, are zeroed. This way, the ECG artifacts are eliminated, and larger signal components, i.e. muscle activity, in the same frequency band, are not affected. The resulting effects of this wavelet thresholding is seen in Figure 3.9. The ECG components in the signal are attenuated whilst the frequency spectrum remains similar to its unfiltered counterpart.

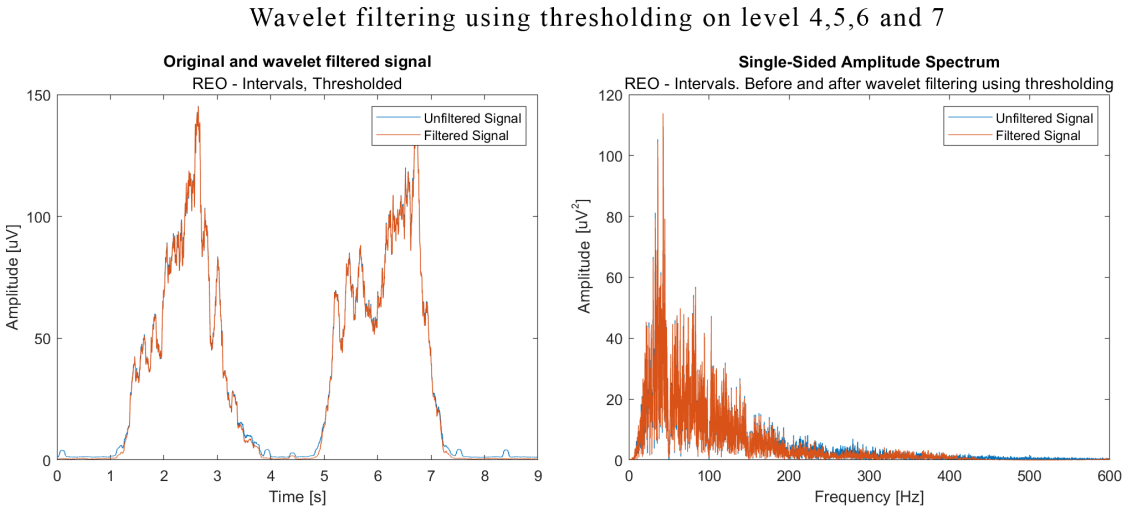

Figure 3.9: Effects of wavelet filtering when thresholding level 4, 5, 6 and 7. The amplitude of the time-domain signal is maintained, the ECG artifacts are attenuated, and the frequency spectrum within the sEMG bandwidth is preserved. The measurement is of a right exterior oblique (REO) muscle.

Considering the benefits and drawbacks of all presented approaches, approach 3 was chosen. This was due to the fact that this approach does not affect the signal frequency spectrum as severely as the other alternatives whilst still attenuating ECG artifacts.

To denoise the signal further, the detail coefficients in level 1 and 2 of the wavelet decomposition were zeroed. These detail coefficients contain high-frequency bandwidth components around 450Hz and higher. As discussed in subsection 2.4.5, these frequencies are above the sEMG frequency spectrum.

3.4 Experiment Structure

The authors of this study acted as test subjects. Both subjects were women, had normal body mass index, and were 25-28 years old. The subjects were few due to

the covid-19 pandemic and the fact that the measurements were early stage testing. Further testing on other subjects would require regulatory approval.

Before conducting the experiments, the skin under the electrodes was exfoliated and cleaned. The electrodes were placed according to Figure 3.1, as discussed in section 3.1. During all experiments, the subjects were in a supine position. To collect relevant data, the experiments consisted of five different tests:

- Relaxation
  - Subject is completely relaxed.
  - Serves as an indicator of how much background noise is present, i.e. if the electrode placement is satisfactory.
  - Used to determine the threshold in the wavelet ECG removal algorithm.
  - Used in the comparison with existing research regarding the characteristics of peritonitis.
- Abdominal tension
  - Subject tenses the abdominal region.
  - Indicates the voltage that a voluntary contraction generates.
- Intervals
  - Subject contracts the abdominal muscles in time intervals.
  - Serves as a comparison between muscle activity during rest and contraction.
- Coughing
  - Subject coughs.
  - Shows rapid contraction of the abdominal muscles that would be present during a cough test.
  - Used in the comparison with existing research regarding the characteristics of peritonitis.
- Breathing deeply
  - Subject is asked to breathe deeply using the abdominal muscles.
  - Generates low-amplitude muscle activity when the oblique muscles contract during exhalation.

4

Results

This section presents all generated results. Firstly, the finished prototype is displayed and explained. Secondly, the effects of the signal processing described in the method section is presented. Lastly, the data gathered during the different tests are displayed and analyzed.

4.1 The Prototype

The finalized prototype is shown in Figure 4.1. The circuit is built into a plastic box made for enclosing electrical equipment. It has four sEMG inputs and one reference input. To avoid user errors, the different types of inputs are placed on separate sides of the enclosure.

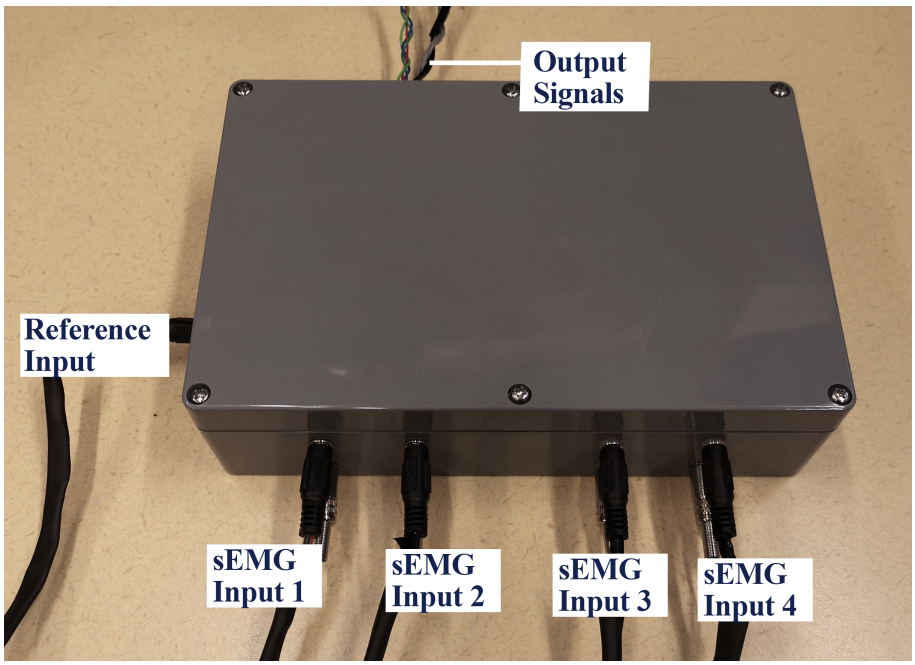

Figure 4.1: The finished prototype.

4.2 Signal Processing

This section presents how the sEMG signal is affected by signal processing. The section is divided into hardware, software and wavelet filtering.

4.2.1 Hardware Filtering

The frequency response of the implemented hardware filters is shown in Figure 4.2. There is a gain of approximately 81dB at the desired bandwidth of the sEMG signal. As can be seen, the frequency response shows steep decline in the gain at frequencies outside of the cut-off frequencies, which is expected.

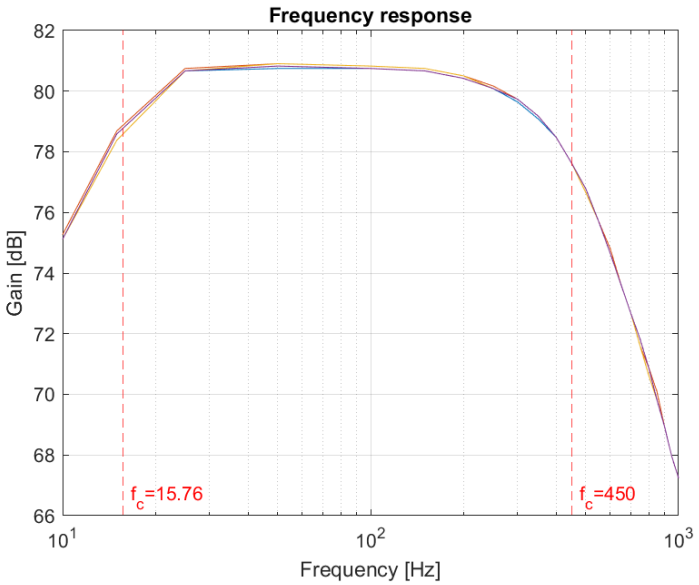

Figure 4.2: The frequency response of each channel of the system. The cut-off frequencies of the high- and low-pass filters are marked with f_c.

4.2.2 Software Filtering

The purpose of implementing digital filters is to remove additional noise and unwanted artifacts. Firstly, the raw data is filtered using a high-pass filter, a low-pass filter, and notch filters, as described in section 3.3. The resulting frequency spectrum of a signal recorded during rest is shown in Figure 4.3. In the unfiltered signal, there is a clear peak at 50Hz due to PLI. There are also harmonics of the 50Hz noise present within the signal at 100Hz, 150Hz, 200Hz, 250Hz, 300Hz and 350Hz. In addition, there is also a peak at 0Hz. In the filtered signal, this peak is no longer present, and the PLI, along with its harmonics, are attenuated.

In the time domain, these filters have the effects shown in Figure 4.4, which depicts a signal recorded during an intervals measurement. The unfiltered signal has a slight offset and a high frequency noise affecting its baseline. The filtered signal has no offset due to the high-pass filtering, and less noise due to the low-pass filtering. The muscle activity is unaffected.

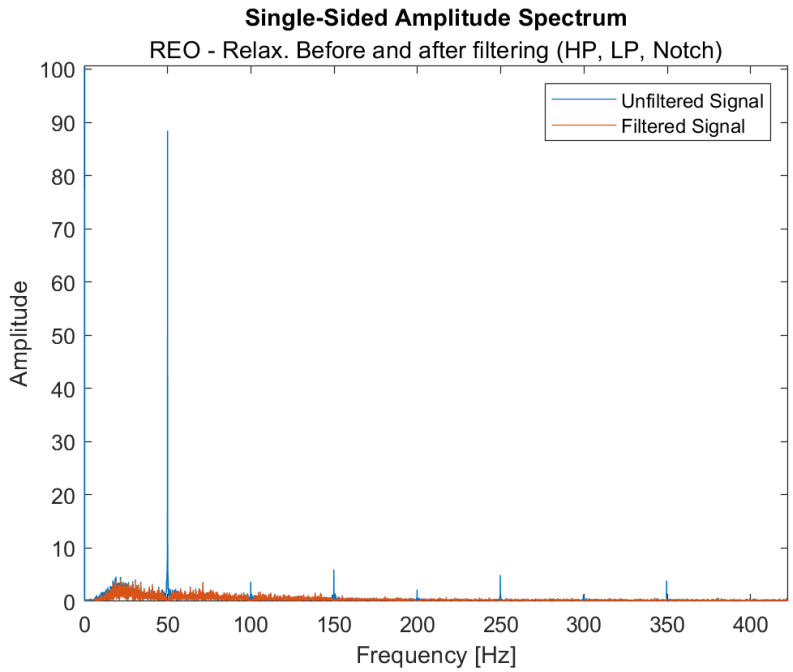

Figure 4.3: Frequency spectrum of a signal recorded on the right exterior oblique (REO) during rest before and after low-pass, high-pass and notch filtering. In the filtered signal, the power line interference is attenuated.

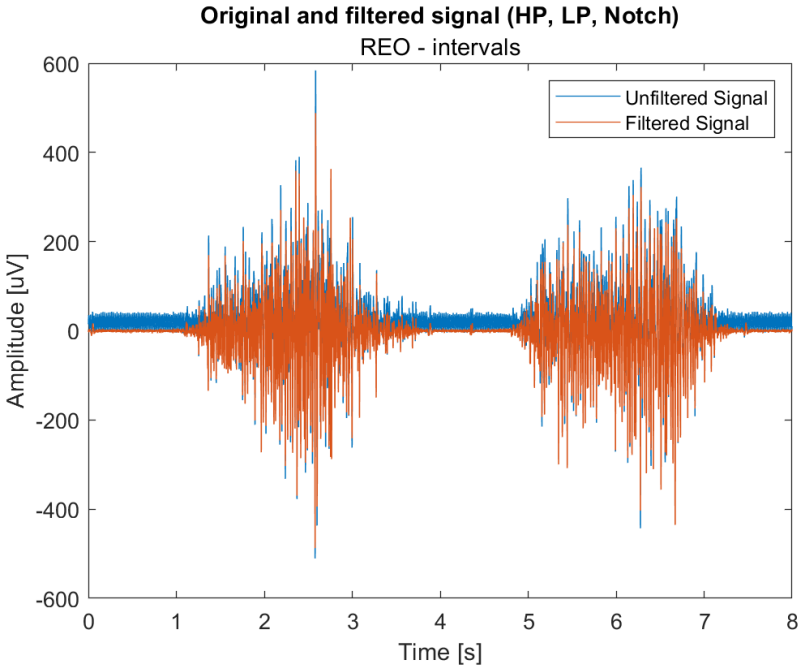

Figure 4.4: Time domain signal before and after filtering with a high-pass, a low-pass and notch filters. The plot shows a signal recorded on the right exterior oblique (REO) during an intervals measurement. Baseline noise, as well as the signal offset, is removed.

The purpose of the wavelet filtering, described in section 3.3, is to remove ECG artifacts and high frequency noise, while maintaining the signal amplitude and envelope characteristics. As can be seen in Figure 4.5, the wavelet filtering attenuates frequencies from ∼430Hz and above. For the measurement shown in the figure, the remaining frequency content is not affected. Furthermore, it can be seen in Figure 4.6 that the signal maintains its amplitude and shape, but the ECG artifacts, as well as much of the baseline noise, are removed.

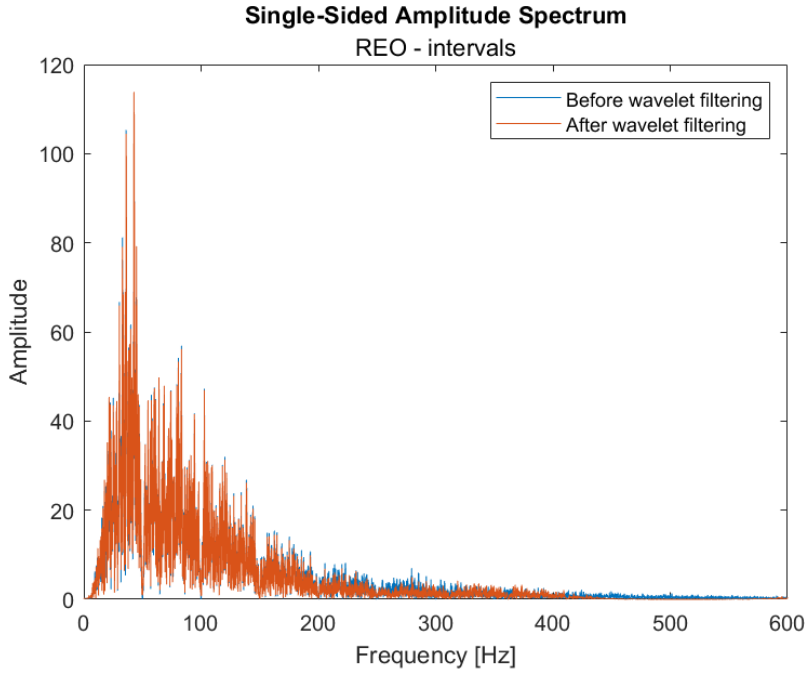

Figure 4.5: The power spectrum of a signal from the right exterior oblique (REO) during an intervals measurement. The plot shows how high frequency components that distort the baseline are attenuated, and that other frequencies are not heavily affected by the wavelet filtering.

In comparison to a signal obtained during an intervals experiment, a signal obtained during breathing has lower amplitude and more prominent ECG artifacts. This means that the ECG artifacts are a bigger part of the entire signal content, compared to a signal with more muscle activity. Accordingly, the part of the power spectrum which originates from the ECG is bigger in a low activity signal. Consequently, the thresholding will attenuate more of the frequency spectrum in a signal with low muscle activity compared to a signal with high muscle activity. This can be seen in Figure 4.7, where not only high frequency components are attenuated, but also frequencies below 100Hz. Since the power spectrum of ECG and EMG signals overlap, the ECG removal affects the EMG signal. However, as seen in Figure 4.8, the ECG and high frequencies are removed, and the effect on the remaining signal in terms of amplitude and shape is minor.

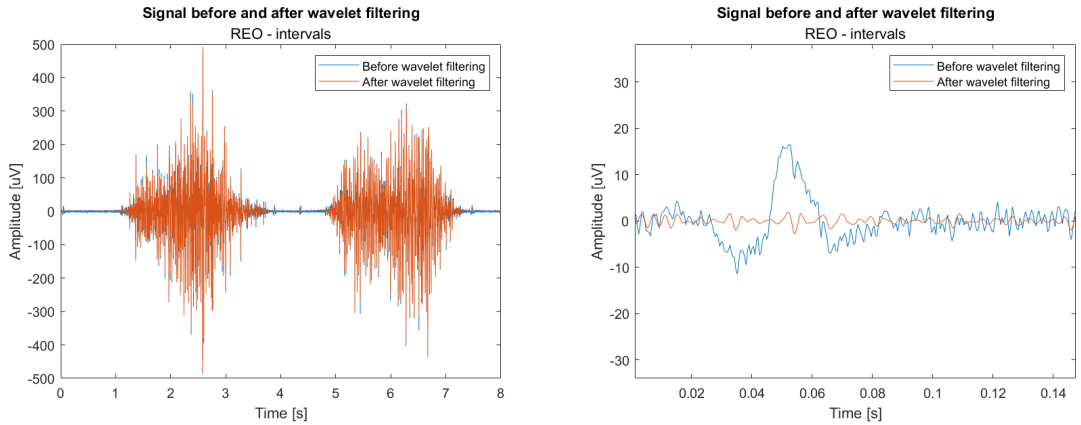

Figure 4.6: A signal of the right exterior oblique acquired during an intervals experiment before and after wavelet filtering. The left plot shows how the signal maintains amplitude and shape. The right plot shows that the baseline is less corrupted by noise, and that the ECG artifacts are attenuated.

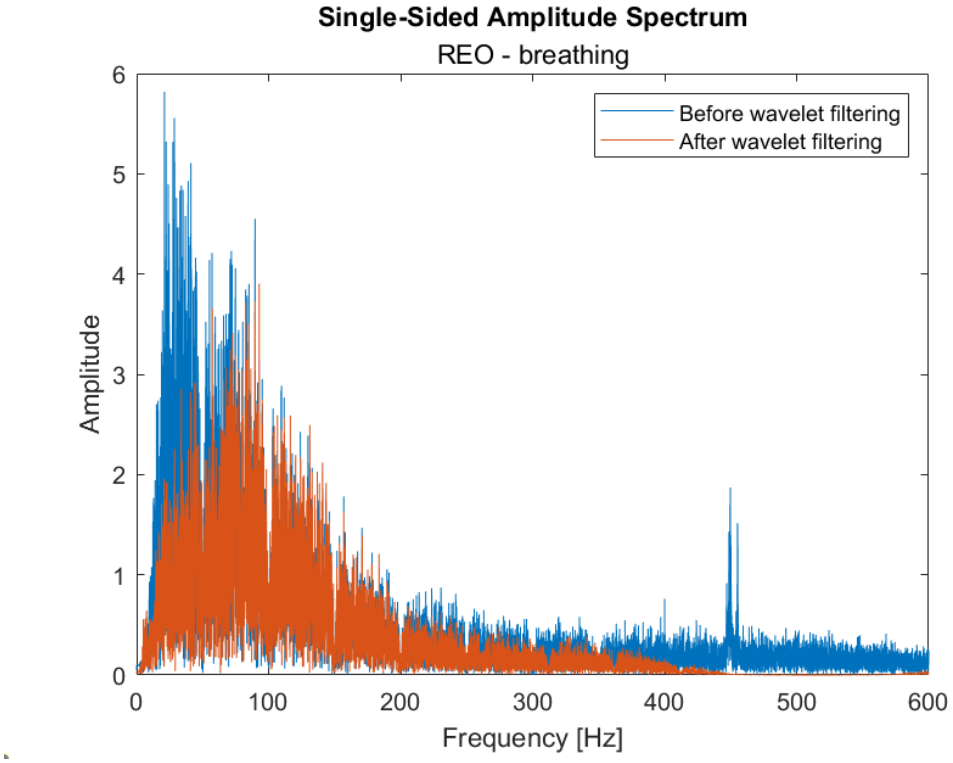

Figure 4.7: Frequency spectrum of a signal recorded during deep breathing from the right exterior oblique (REO). High frequencies are attenuated to avoid baseline distortion and low frequencies are attenuated to remove ECG components.

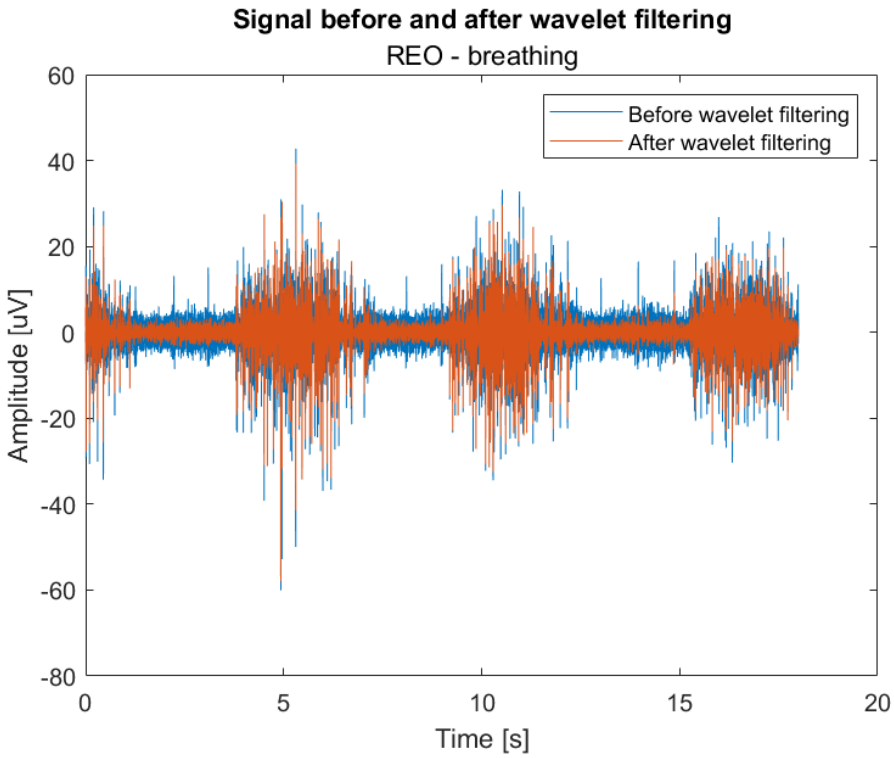

Figure 4.8: Signal recorded during deep breathing from the right exterior oblique (REO), before and after wavelet filtering. After filtering, the ECG artifacts and the high frequency noise are attenuated. The part of the signal that corresponds to muscle activity is not considerably affected.

4.3 Measurements

This section presents the measurements made using the presented prototype. The measurements were acquired from the internal and external oblique muscles during relaxation, tension, intervals, coughing and deep breathing. The results are compared between the two subjects as well as to the conclusions made by Rozin and Meyer [6].

4.3.1 Relaxation

The resulting measurements of subject 1 and 2 during complete relaxation in a supine position is presented in Figure 4.9. As can be seen, there are slight amplitude differences between different muscles as well as between the two subjects. The recorded signals from both subjects range from 0.5-2μV. This result is somewhat counterintuitive, considering that there should be no muscle activity. Clearly, there is some noise present. However, some background is expected in most sEMG applications [20].

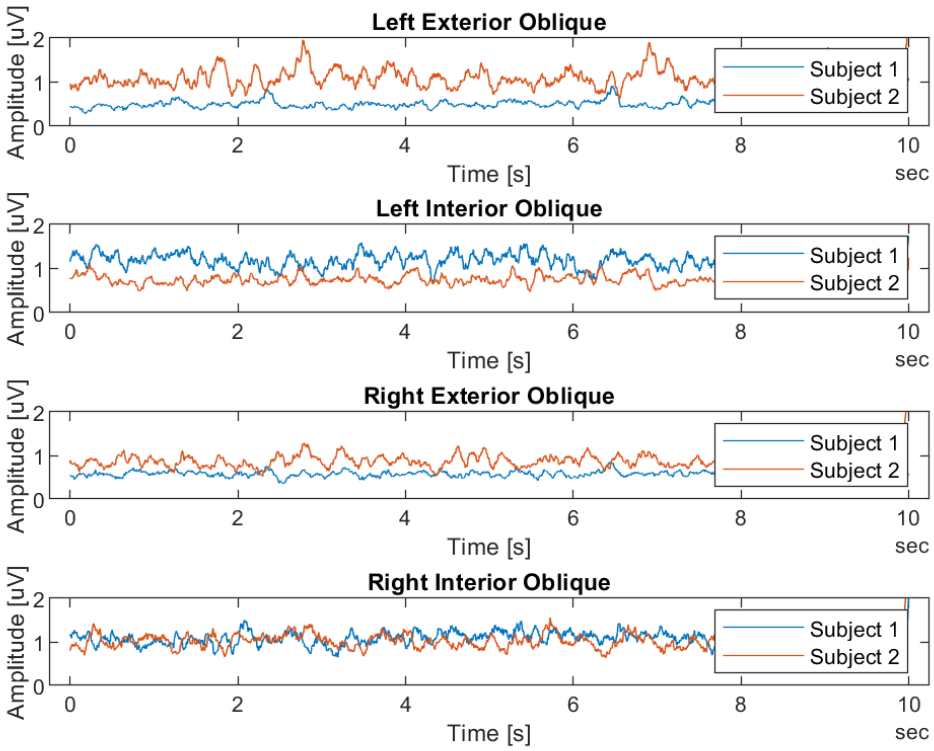

Figure 4.9: Measurements during relaxation of each abdominal quadrant of both subjects. There is a slight difference in amplitude between subject 1 and 2.

As presented in section 2.6, the resting activity of a patient suffering from peritonitis is approximately 22% of a voluntary contraction of a healthy subject. To illustrate

the prototype's ability to detect hypothetical muscle activity caused by peritonitis, 22% of healthy muscle activity while contracting the muscles, together with signals recorded from healthy individuals at rest, are depicted in Figure 4.10. Both measurements are recorded during the same session, i.e. using the same electrodes, subject and position. As seen in Figure 4.10, there is a clear difference between signals recorded during rest and 22% of the amplitude of signals recorded during voluntary contractions. Signals recorded during rest in the healthy subjects are in the range of 0.5-2μV, whilst the range of the signals containing hypothetical peritonitis varies between approximately 10-50μV. The measured voluntary contraction strength varies between subjects, measurement sessions and electrode positions. But nevertheless, the prototype can distinguish between resting muscle activity from healthy individuals and hypothetical activity caused by peritonitis.

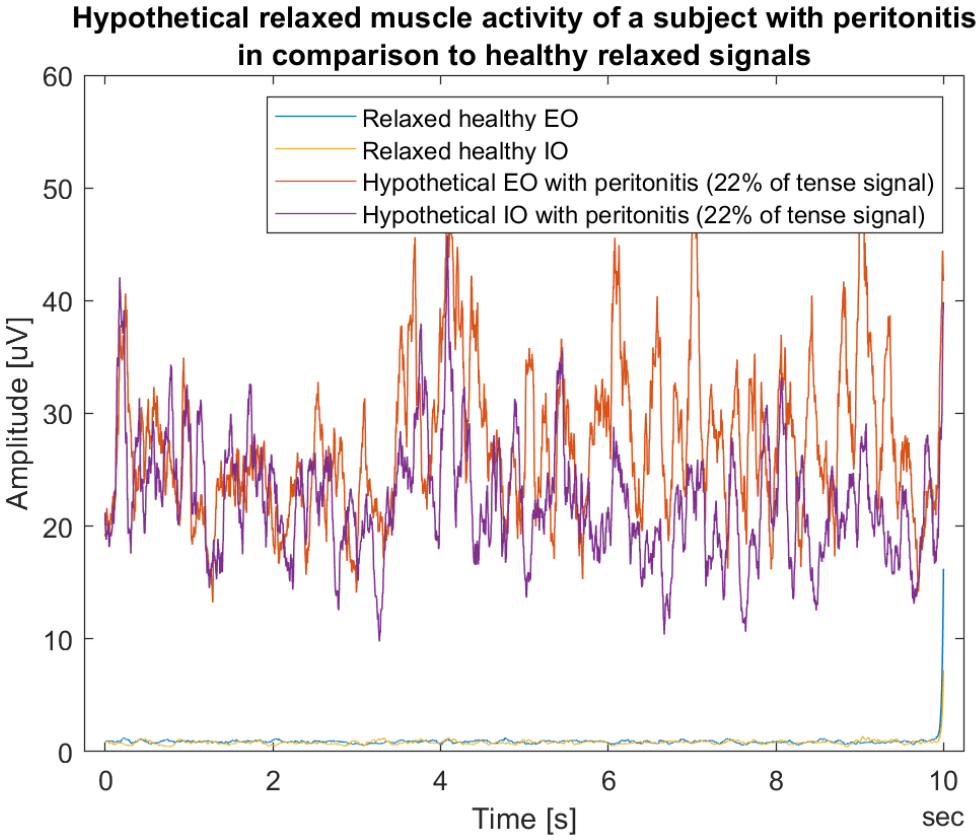

Figure 4.10: Hypothetical abdominal activity during rest of a subject with peritonitis in comparison to a healthy subject. According to [6], the muscle activity of a patient with peritonitis is approximately 22% of a voluntary contraction. The measurements are of an exterior oblique (EO) and an interior oblique (IO) muscle.

4.3.2 Tension

The measurements of both subjects during voluntary abdominal muscle contraction can be seen in Figure 4.11. The recorded amplitudes are in the range of 25-175μV. The amplitudes of both subjects are similar, apart from the left interior oblique for

which subject 1 has a higher amplitude. The signals in this figure can be compared with the signals in Figure 4.9, which shows that all signal amplitudes are greater during tension than during rest. As previously stated, the measured voluntary contraction strength varies between subjects, measurement sessions, and electrode positions.

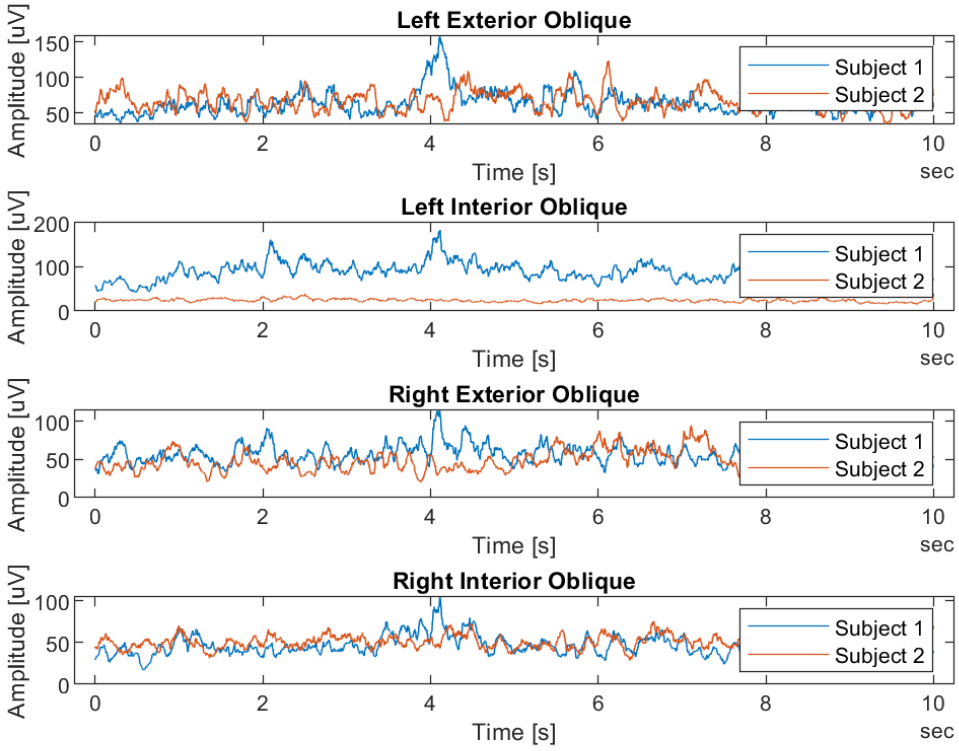

Figure 4.11: Measurements during tension of each abdominal quadrant. There are amplitude differences between the subjects and between the different muscles.

4.3.3 Intervals

Two interval measurements, acquired two different days, of subject 1 and 2 can be seen in Figure 4.12 and Figure 4.13. For both subjects, there are apparent amplitude differences between the measured muscles. Furthermore, there are differences in measured amplitude on the same muscles on different days. This is to be expected, as the subjects had no feedback on the contraction strength. Nevertheless, for all measurements, there is a clear difference between abdominal tension and relaxation for both subjects. In both figures, electrical silence can be observed between the muscle tension intervals.

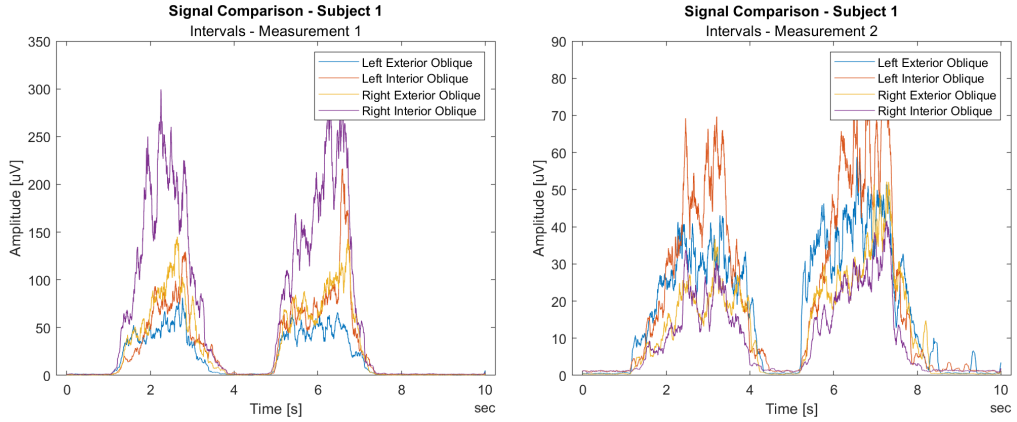

Figure 4.12: Recordings of subject 1 over two different measurement sessions. There is a distinct difference in signal amplitudes between the two measurements.

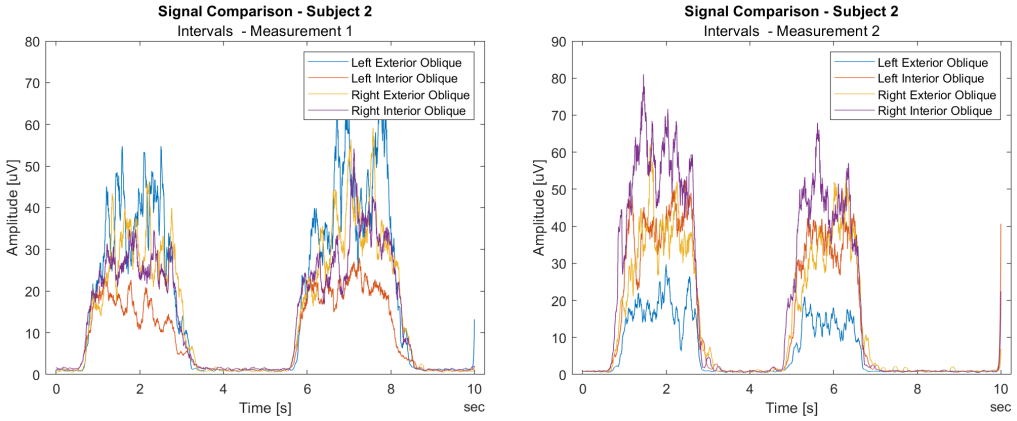

Figure 4.13: Recordings of subject 2 over two different measurement sessions. There is a difference in signal amplitudes between the two measurements.

4.3.4 Cough test

The sEMG measurements of subject 1 and subject 2 recorded during a cough can be seen in Figure 4.14 and Figure 4.15. The figures show cough activity, which lasts for 200-300ms and has amplitudes between 100-500μV, followed by electrical silence. The end of the cough, which is marked in the figures, was found by visual inspection of the plots.

As described in section 2.6, a patient with peritonitis would have residual electrical activity for 200ms after the initial cough activity [6]. This is illustrated in Figure 4.16, where 23% of the amplitude of a muscle signal recorded during healthy voluntary contraction is visualized where the residual activity could be expected. The percentage is an estimation based on the findings by [6]. It is apparent from these figures that the prototype can measure the abdominal muscle activity during a cough, and that it displays electrical silence if no guarding is present.

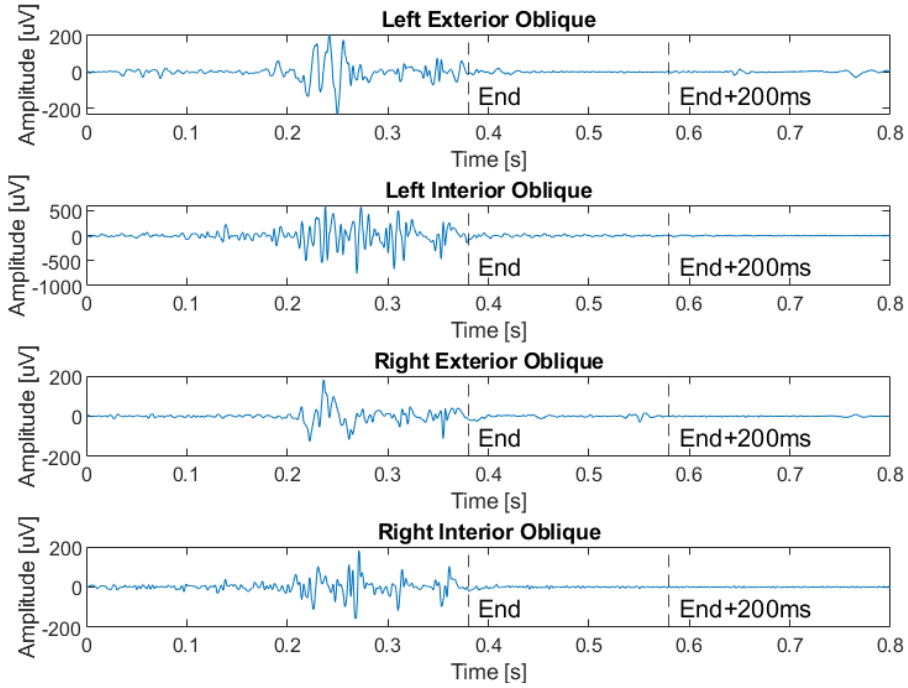

Figure 4.14: Measurements of subject 1 during a cough test. The plots show electrical cough activity for ∼200ms followed by electrical silence.

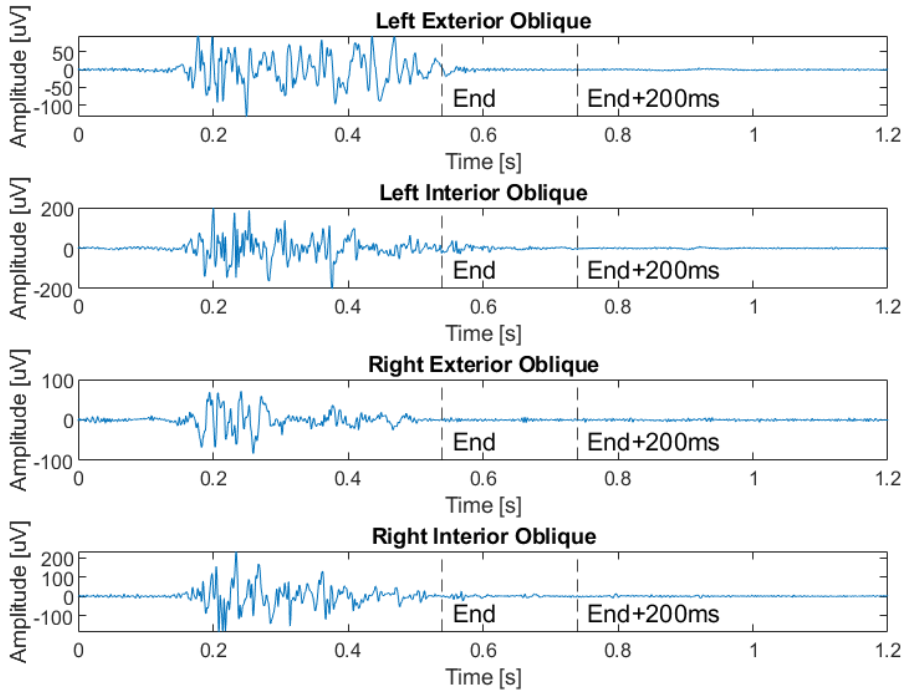

Figure 4.15: Measurements of subject 2 during a cough test. The plots show electrical cough activity for ∼300ms followed by electrical silence.

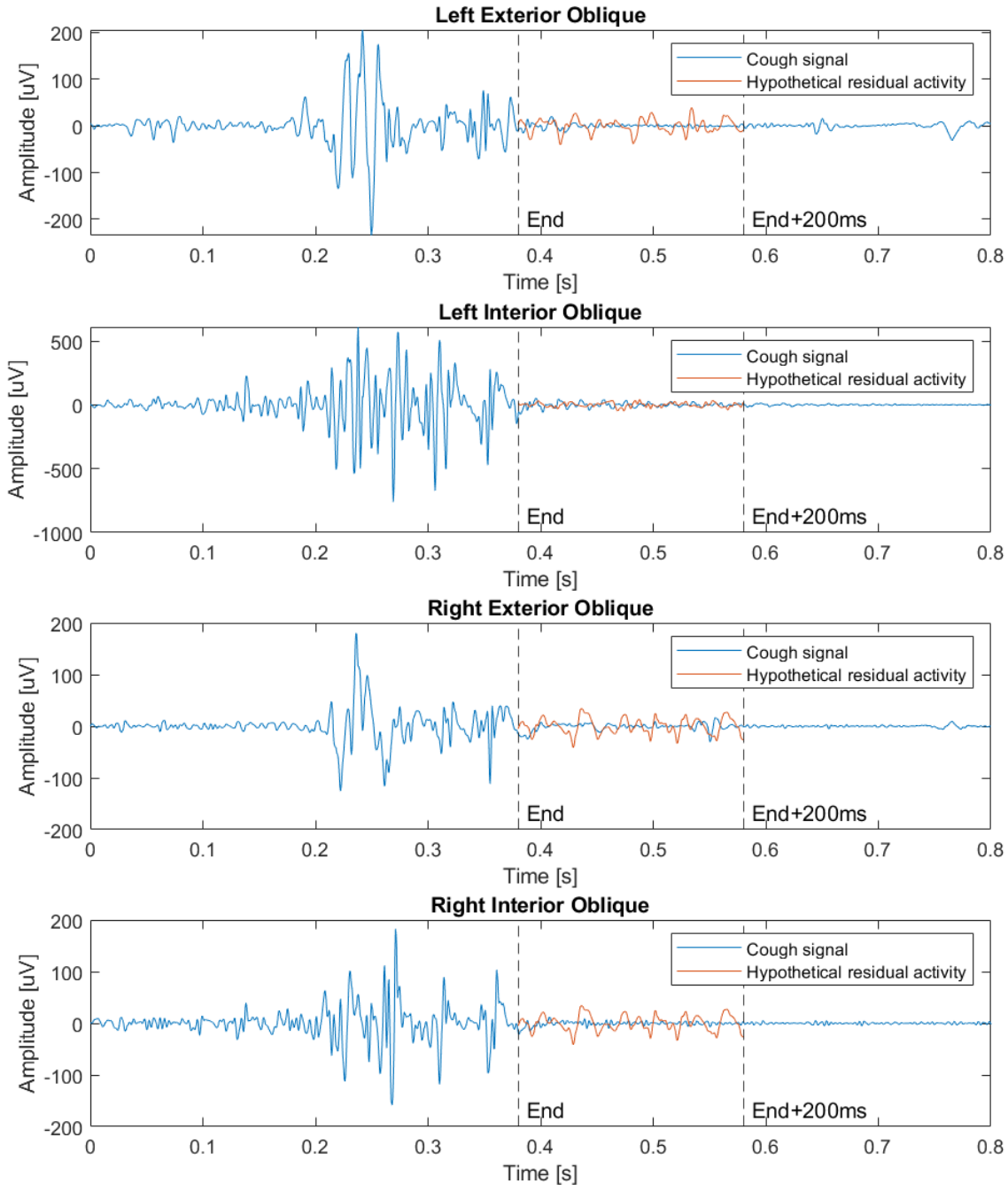

Figure 4.16: Cough activity from subject 1 displayed together with a hypothetical residual activity to visualize how guarding could appear in the signals. The hypothetical residual activity is based on the findings by [6].

4.3.5 Breathing

The results of the breathing experiments of both subjects are shown in Figure 4.17 and Figure 4.18. These figures show that the prototype can measure oblique muscle activity with amplitude $\leq 5\mu$V. During these measurements, both subjects consciously breathed deeply and focused on using the abdominal region instead of the chest area. These figures can be compared with Figure 4.9 which depicts signals recorded during rest. During the acquisition of these signals, both subjects were breathing normally. However, this does not appear in the measurements. Taken together, these results suggests that deep, conscious breathing is necessary to generate activity that the prototype can detect. There is an increased muscle activity during exhalation in both the exterior and interior oblique muscles. Subject 2, as seen in Figure 4.18, has some additional activity in the exterior oblique measurements during inhalation marked in red.

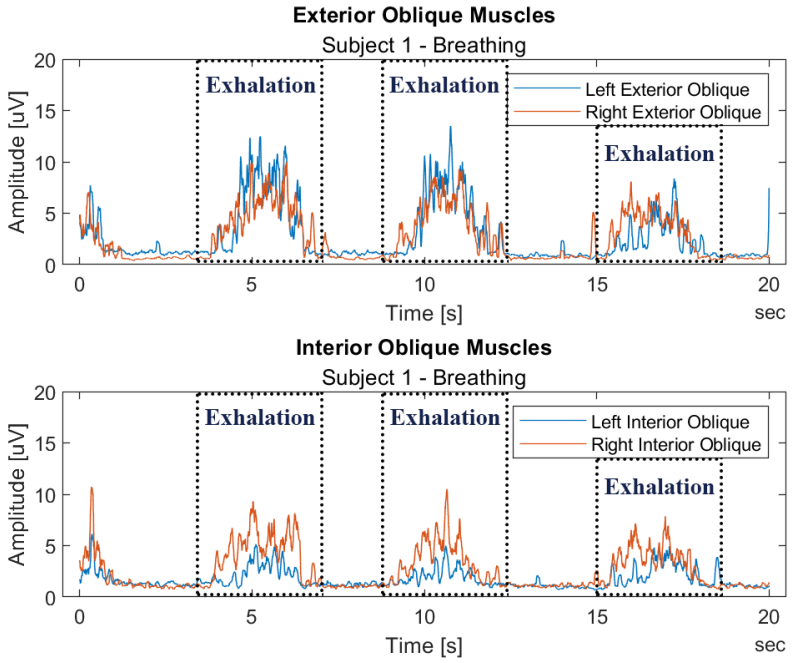

Figure 4.17: Subject 1 breathing deeply. There is an increased abdominal activity during exhalations in the exterior and interior oblique muscles.

The purpose of the breathing experiments was to investigate whether the prototype could measure small abdominal muscle activity. Figure 4.17 and Figure 4.18 clearly show that it is able to do so. To put these findings in relation to the findings by [6], a hypothetical signal representing guarding is put in comparison to signals recorded on a healthy subject during breathing, as seen in Figure 4.19. As can be seen, the prototype can detect smaller muscle activity than that which would be hypothetically introduced by peritonitis.

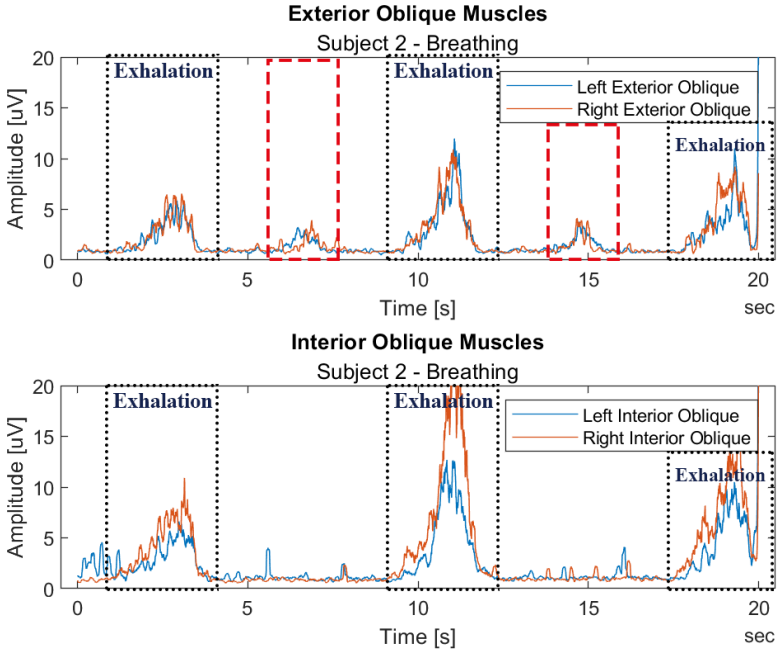

Figure 4.18: Subject 2 breathing deeply. There is an increased abdominal activity during exhalations in the exterior and interior oblique muscles. There is some extra abdominal activity recorded in the exterior oblique muscles between exhalations, marked in red.

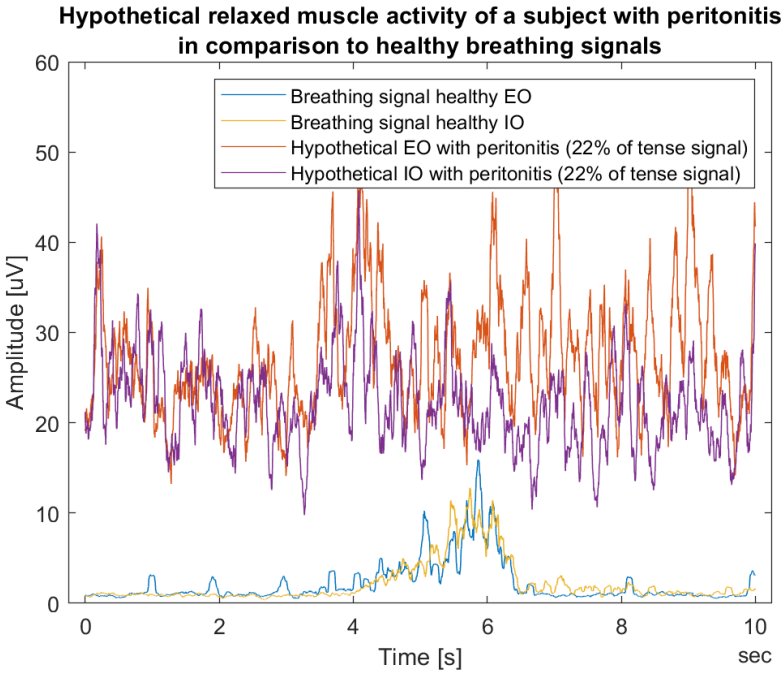

Figure 4.19: Comparison of healthy breathing activity and hypothetical resting activity present in patients suffering from peritonitis. The measurements are of an exterior oblique (EO) and an interior oblique (IO) muscle. The hypothetical signal has higher amplitude.

5
Discussion

The aim of this thesis was to create a prototype of a device that uses sEMG to acquire abdominal muscle activity. The future purpose of the device is to be able to diagnose peritonitis by detecting guarding in the abdominal muscles. Using the prototype, we conducted several experiments to evaluate its performance in regards to detecting small changes in muscle tension. The acquired data from these experiments were then compared with similar, existing research.

5.1 Hardware and Signal Processing

The finished prototype is able to measure on all four quadrants simultaneously, namely on the internal and external oblique muscles, with sufficient sensitivity and quality. This means that the device can detect small muscle activity, such as deep breathing, as well as rapid muscle tension during coughing. It also means that noise, for instance ECG artifacts and PLI, are sufficiently attenuated without compromising the signal quality. The ECG removal was achieved through developing a wavelet thresholding algorithm. The algorithm attenuates detail coefficients using a threshold that is based on ECG components in a reference signal. Our study suggests that, by using this method, the frequency spectrum is less compromised compared to attenuating all frequencies within the ECG bandwidth. With this method, we believe that we can remove the ECG without affecting the parts of the signal containing abdominal muscle activity. Given the fact that the aim of this thesis was to create a prototype and generate data which could serve as a basis for future developments, we believe that using notch filters to remove PLI, despite how they affect the waveform of the sEMG signal, is acceptable. However, for future iterations, we see a need to investigate other possible solutions.

5.2 Peritonitis in sEMG Recordings

As discussed in section 2.2, it is well known that peritonitis causes an increased abdominal muscle activity called guarding. This abdominal rigidity is a key factor in diagnosing peritonitis via palpation. However, few studies have been done using sEMG to measure and analyze this abdominal rigidity. Throughout the course of this project, we were only able to find one relevant study on this topic [6]. Said study is from 1973 and does not disclose details regarding signal processing or measurement

set-up. The electrode placement in that study is not in accordance to today's standards and recommendations. Consequently, our measured data, and that study's data is different, mainly in regards to amplitude. To be able to compare our findings with that study, we have assumed that the relation between healthy activity and activity generated by abdominal guarding found in the study is valid. This is an assumption, and more studies are needed to validate these characteristics. Therefore, a note of caution is due when interpreting the findings in our figures depicting hypothetical peritonitis in comparison to healthy subjects. Having said that, despite the fact that the previous research, on which we base our conclusions, is very limited, the found study showed very promising results.

5.3 Measurements & Findings

The measurements acquired during rest, as seen in Figure 4.9, are in the range of 1-2μV. This means that the baseline signal, during electrical silence, is not zero. This may be due to many reasons, such as cross-talk from active muscles, noise generated at the skin/electrode interface, and PLI. However, this baseline noise is very low and does not affect the signal once abdominal muscle activity is detected. We therefore deem the baseline noise acceptable. The noise of the baseline signal varies between the two subjects. We believe that this variation is due to difference in electrode placements and amount of adipose tissue of the subjects. As discussed in subsection 2.4.4, there is a consensus that electrodes should be placed in parallel to the muscle fiber orientation. As we observed during our experiments, if an electrode pair was placed poorly in relation to the muscle fiber orientation, the baseline noise was high and muscle activity was recorded poorly. We want to emphasize that to acquire useful data, it is of the utmost importance that the electrode placement is correct.

The measurements of tense muscles, as seen in Figure 4.11, are generally in the range of 25-175μV. This amplitude variety is due to difference in individual contraction strength and electrode placement. When observing the signal from the left interior oblique, one can see that the amplitude of subject 2 is significantly lower compared to other muscles and subject 1. This inconsistency highlights the importance of a correct electrode placement to achieve high amplitude signals. Nevertheless, in all signals, we see a clear distinction between muscle activity during rest and contraction, as illustrated by the intervals experiments seen in Figure 4.12 and Figure 4.13.

If we now turn to the results of the deep breathing experiments, a clear distinction between relaxation and small muscle movements can be seen in Figure 4.17 and Figure 4.18. It is apparent from these figures that both the interior and exterior obliques are activated during exhalation. The purpose of the breathing experiments was to determine whether the prototype was sensitive enough to pick up very small muscle signals. As shown, breathing can be detected. However, it is very important to consider that the breathing measurements are of very conscious deep breaths using the abdominal region. Normal breathing, which is present in the relaxation measurements, does not appear in the signal. This indicates that there is a limit

to the sensitivity of the prototype, but we also believe that it may be due to the fact that the obliques are not engaged as much during shallow breathing. As seen in, Figure 4.18, there is extra activity in the exterior oblique muscles in between exhalations. We believe that this is due to cross-talk caused by the diaphragm as it activates during deep inhalation. It is therefore important to acknowledge that cross-talk is present. However, we have only been able to identify cross-talk during very deep inhalations. As discussed in the theory, large IED increases the risk of cross-talk. As the IED in the experiments was larger than the recommendations, we see a possibility that the cross-talk can be avoided with smaller electrodes and IED. Unfortunately, we were not able to acquire electrodes that matched our preferences during this project, as discussed in section 3.2.

To diagnose peritonitis, the cough test is used to determine rigidity and pain levels. In case of peritonitis, a patient may experience a cough as very painful and the abdominal muscles will have increased tension after it. By measuring the abdominal muscle activity during a cough with our prototype, we wanted to compare measurements on healthy subjects with the results reported by [6]. In that study, patients with peritonitis show residual abdominal activity after a cough with a duration of $\sim$ 200ms. In our measurements, seen in Figure 4.14 and Figure 4.15, the end of the cough has been marked by visually looking at the plots. In the case of peritonitis, we believe that marking the end of the cough would be more difficult. However, we also presume that the duration of the electrical activity would be prolonged. According to these suggestions, we can infer that the duration of the cough could be used as an indication of peritonitis. The main goal of the cough experiments was to determine if the prototype can sufficiently record rapid contractions. These figures clearly show that it can measure and display the forceful and rapid cough contraction, as well as the electrical silence that follows.

To draw conclusions about whether the prototype could detect peritonitis, the amplitude ratio between a voluntary contraction and the amplitude generated by guarding, shown in [6], has been used. This ratio was applied to our data to generate the hypothetical signals seen in Figure 4.10, Figure 4.16, and Figure 4.19. The contrast between a healthy and a theoretically ill patient's muscle activity is clearly distinguishable in these figures. Therefore, we believe that our prototype has sufficient sensitivity to differentiate between guarding and healthy signals. However, with a small number of subjects and limited research to compare with, caution must be applied when interpreting the results.

5.4 Limitations

To use sEMG to measure the external and internal obliques to detect peritonitis is not well researched. Therefore, we can only estimate how peritonitis would appear in the sEMG measurements using the one study that was found. This is very limiting. In addition, the methodology used in that study compared to ours is different in regards to electrode placement. Furthermore, no information regarding signal processing, hardware, PLI-reduction, measurement position or instrumentation is

disclosed. We are aware of the fact that this is not an ideal study to compare our data with. Despite these limitations, we believe that it is exciting to investigate an unexplored field where there is a lot of possibilities for further research and advancements. To make more informed conclusions regarding the final product's feasibility, further studies are needed to investigate how the characteristics of peritonitis manifests in sEMG measurements.

The methodology used within this thesis is also limited. The number of subjects were few and very homogeneous. Therefore, more data is needed to thoroughly assess the performance of the prototype. A larger and more diverse subject group would be necessary to properly evaluate the prototype's functionality. This would include subjects with different BMI, sex and age. It is known that the amount of adipose tissue affects the sEMG signal, and therefore, studies are needed to confirm that the prototype performs as intended on diverse subjects. Furthermore, to verify the prototype's intended functionality, a clinical study on patients suffering from peritonitis is needed. Moreover, due to the covid-19 pandemic and limited project budget, our choice of components and electrodes was fairly limited.

5.5 Future Developments

The prototype can clearly differentiate between abdominal muscle activity and relaxation, and it has sufficient sensitivity to detect small muscle activity. However, further studies are required to improve the prototype. For example, it would be of interest to investigate to what degree cross-talk is present within the recorded signals. The conducted experiments only measured abdominal tension when all external and internal oblique muscles are activated voluntarily and simultaneously. Future studies could assess whether separate excitation of the muscles generates a response in neighbouring quadrants. This response could indicate if cross-talk is present. If this study would be performed, it could show if localized peritonitis can be detected and assigned to a specific quadrant.

The aim of this thesis was to create a first prototype to collect proof-of-concept data. In future iterations, several developments and improvements can be made to make it more sophisticated and robust. For example, the developed wavelet-algorithm, at times, misses some ECG artifacts. We believe that this may be due to poorly recorded reference signals. To make the ECG removal more robust, adaptive filters could be a viable option [42]. Furthermore, if real time displaying of the signal is desirable, wavelet-filtering may require too much computation power. Moreover, an investigation of whether the entire EMG spectral content is needed to detect small muscle contractions would be of interest. If such an investigation would conclude that more spectral content can be removed without attenuating information required to detect peritonitis, the prototype could be optimized and simplified.

Further studies and developments are required to establish the viability of the final product. For example, it is obvious by looking at Figure 4.1 that a future device would need a better and sleeker design. Since this is an initial prototype, the ap-

pearance and design was not prioritized. Another example is the data acquisition, which can be simplified to improve user experience. Currently, all analog inputs must be connected to an NI ELVIS II+ platform. In the finished product, it would be desirable to be able to process and display the signals independent from other devices. This can be done by implementing, for example, an A/D converter and microprocessor into the circuit. To further improve the user experience, fixed electrode pairs with small IED could be used. This would simplify the electrode placement process, and thus, improve measurements and repeatability. Moreover, we believe that enabling real-time displaying of the muscle activity is beneficial for the user when interpreting the data.

5.6 Summary

The result of our research shows that the created prototype can distinguish between muscle tension and relaxation with sufficient sensitivity and resolution. It can measure oblique muscle activity during small contractions, such as those generated by breathing, and rapid contraction, such as during a cough. The combination of our findings with the findings of Rozin and Meyer provides some support for the conceptual idea that the created prototype can detect peritonitis. However, to develop a full picture of the product's feasibility, additional studies will be needed. We believe that one significant future study is a clinical study on patients suffering from peritonitis with the aim to verify the characteristics described by Rozin and Meyer. Moreover, we believe that conducting experiments on a more diverse population is critical to determine the product's viability.

6
Conclusion

This project was undertaken to design a prototype which measures sEMG on the abdominal muscles, and evaluate whether it could be used to indicate the presence of peritonitis. Peritonitis can be identified by increased activity in the abdominal muscles, as it indicates guarding. The developed prototype measures muscle activity of the internal and external obliques on both sides simultaneously. It does so by using four electrode pairs that share reference electrode. The created prototype was successful in detecting and differentiating between muscle relaxation and excitation. The most important limitations lies in the fact that the subjects were few, that no measurements could be done on patients suffering from peritonitis, and that research on how peritonitis appears in sEMG recordings is extremely limited. Notwithstanding these limitations, the study suggests that the prototype has sufficient sensitivity to distinguish small muscle activity, such as guarding, in all four abdominal quadrants.

This study has found that generally, oblique muscle signals recorded during rest are in the range of 0.5-2μV, whilst signals recorded during voluntary contraction are in the ranges of 25-175μV. With the measurements acquired with the prototype, a user can clearly distinguish between muscle activity and relaxation. The sEMG amplitude varies depending on subject and electrode position. Therefore, it is of great importance that the electrodes are placed appropriately, namely in the direction of the muscle fiber orientation, to generate relevant measurements.

Another aim of this research was to examine whether the prototype could measure small abdominal muscle signals, such as those generated by breathing. No muscle activity was detected during "normal" breathing, meaning when the subjects were not deliberately breathing with the abdomen. This finding suggest that the exterior and interior oblique are not activated during normal breathing, or possibly, that the prototype is not sensitive enough. However, the experiments showed that the prototype can measure breathing when the abdominal muscles are consciously engaged. The peaks of these signals, acquired during deep breathing, range from 5-15μV and are clearly distinguishable.

The conclusions that can be drawn from the only study available on the characteristics of peritonitis in sEMG recordings, is that muscle activity caused by peritonitis is detectable in relaxation, after cough and during palpation. During relaxation, peritonitis generates a heightened abdominal muscle activity that corresponds to $\sim 22\%$ of the amplitude from a healthy voluntary contraction. The study also sug-

gests that, in sick patients, residual electrical activity is present after coughing and palpation. Even though this study has many limitations, it showed promising results in diagnosing peritonitis by analyzing these characteristics.

The results of our research supports the idea that, if the study found regarding the characteristics of peritonitis in sEMG is reliable, the prototype can detect said characteristics. Despite these promising results, questions remain. More studies are required to verify how peritonitis manifests in the oblique muscle activity. Furthermore, studies investigating how cross-talk influences the measurements are needed. This is due to that the breathing experiments showed that cross-talk from the diaphragm may affect the external oblique signals. Moreover, clinical studies, as well as user-interface and usability improvements are required to realize a feasible product.

In conclusion, our study contribute in several ways to our understanding of the feasibility of a device which can aid in diagnosing peritonitis using sEMG. The built prototype provides a basis for future developments. The experiments has confirmed that it can measure relevant muscle activity with sufficient sensitivity. With that said, more studies are required, but despite that fact, we believe in the potential this product has in the medical field.

Bibliography

[1] C. Macaluso and R. McNamara, "Evaluation and management of acute abdominal pain in the emergency department," *International Journal of General Medicine*, vol. 2012, no. 5, pp. 789–797, Sep. 2012, ISSN: 1178-7074. DOI: 10.2147/IJGM.S25936. [Online]. Available: http://www.dovepress.com/evaluation-and-management-of-acute-abdominal-pain-in-the-emergency-dep-peer-reviewed-article-IJGM (visited on 21/01/2021).

[2] R. Skipworth and K. Fearon, "Acute abdomen: Peritonitis," *Emergency Surgery*, vol. 26, no. 3, pp. 98–101, Mar. 2008, ISSN: 02639319. DOI: 10.1016/j.mpsur.2008.01.004. [Online]. Available: https://linkinghub.elsevier.com/retrieve/pii/S0263931908000185 (visited on 21/01/2021).

[3] G. J. Tortora and B. Derrickson, *Introduction to the human body*, 10th ed. Hoboken, NJ, USA: John Wiley & Sons, 2014, ISBN: 978-1-118-88407-2.

[4] A. W. Kastelein, L. M. Vos, K. H. de Jong, J. O. van Baal, R. Nieuwland, C. J. van Noorden, J.-P. W. Roovers and C. A. Lok, "Embryology, anatomy, physiology and pathophysiology of the peritoneum and the peritoneal vasculature," *Seminars in Cell & Developmental Biology*, vol. 92, pp. 27–36, Aug. 2019, ISSN: 10849521. DOI: 10.1016/j.semcdb.2018.09.007. [Online]. Available: https://www.sciencedirect.com/science/article/abs/pii/S1084952118300193 (visited on 21/01/2021).

[5] J. T. Ross, M. A. Matthay and H. W. Harris, "Secondary peritonitis: Principles of diagnosis and intervention," *BMJ (Clinical research ed.)*, vol. 361, no. k1407, Jun. 2018, ISSN: 1756-1833. DOI: 10.1136/bmj.k1407. [Online]. Available: https://pubmed.ncbi.nlm.nih.gov/29914871/ (visited on 21/01/2021).

[6] R. R. Rozin, S. Meyer and R. Rozin, "Electromyography of Anterior Abdominal Muscles: During Diffuse and Localized Peritonitis," *Archives of Surgery*, vol. 106, no. 2, pp. 160–163, Feb. 1973, ISSN: 0004-0010. DOI: 10.1001/archsurg.1973.01350140026009.

[7] A. Merlo and I. Campanini, "Technical Aspects of Surface Electromyography for Clinicians," *The Open Rehabilitation Journal*, vol. 3, no. 1, pp. 98–109, Jan. 2010, ISSN: 18749437. DOI: 10.2174/1874943701003010098. [Online]. Available: http://benthamopen.com/ABSTRACT/TOREHJ-3-98 (visited on 26/01/2021).

[8] J. Wang, L. Tang and J. E Bronlund, "Surface EMG Signal Amplification and Filtering," *International Journal of Computer Applications*, vol. 82, no. 1, pp. 15–22, Nov. 2013, ISSN: 09758887. DOI: 10.5120/14079-2073. [Online]. Available: https://www.researchgate.net/publication/260845647_Surface_EMG_Signal_Amplification_and_Filtering (visited on 21/01/2021).

[9] M. A. Malangoni and T. Inui, "Peritonitis – The Western Experience," *World Journal of Emergency Surgery*, vol. 1, no. 1, p. 25, Sep. 2006, ISSN: 17497922. DOI: 10.1186/1749-7922-1-25. [Online]. Available: http://wjes.biomedcentral.com/articles/10.1186/1749-7922-1-25 (visited on 02/02/2021).

[10] S. I. Vas, D. E. Low and D. G. Oreopoulos, "Peritonitis," in *Peritoneal Dialysis: Developments in Nephrology*, K. D. Nolph, Ed., Dordrecht, Netherlands: Springer, 1981, pp. 344–365, ISBN: 978-94-017-2563-7. DOI: 10.1007/978-94-017-2563-7_12. [Online]. Available: https://doi.org/10.1007/978-94-017-2563-7_12.

[11] M. K. Voung and J. S. Sung, Eds., *Liver disease and peritonitis: causes, treatment, and prevention*, ser. Hepatology research and clinical developments. New York, USA: Nova Science Publishers Inc, 2012, ISBN: 978-1619420809.

[12] Blausen, "Medical gallery of Blausen Medical," *WikiJournal of Medicine 1*, vol. 2, ISSN: 2002-4436. DOI: 10.15347/wjm/2014.010. [Online]. Available: https://commons.wikimedia.org/wiki/Category:Human_surface_anatomy_of_abdomen#/media/File:Blausen_0005_AbdominopelvicQuadrants.png (visited on 11/05/2021).

[13] C. M. Ferguson, "Inspection, Auscultation, Palpation, and Percussion of the Abdomen," in *Clinical Methods: The History, Physical, and Laboratory Examinations*, H. K. Walker, W. D. Hall and J. W. Hurst, Eds., 3rd ed., Boston, USA: Butterworths, 1990, ISBN: 978-0-409-90077-4. [Online]. Available: http://www.ncbi.nlm.nih.gov/books/NBK420/ (visited on 02/02/2021).

[14] D. A. Rosenbaum, *Human motor control*, 2nd ed. Amsterdam, Netherlands: Elsevier Inc., 2010, ISBN: 978-0-12-374226-1.

[15] T. Moritani, D. Stegeman and R. Merletti, "Basic physiology and biophysics of emg signal generation," in *Electromyography: physiology, engineering, and noninvasive applications*, R. Merletti and P. Parker, Eds., Hoboken, NJ, USA: Wiley-Interscience, 2004, pp. 1–25, ISBN: 978-0-471-67580-8.

[16] R. Merletti and S. Muceli, "Tutorial. Surface EMG detection in space and time: Best practices," *Journal of Electromyography and Kinesiology*, vol. 49, p. 102 363, Dec. 2019, ISSN: 10506411. DOI: 10.1016/j.jelekin.2019.102363. [Online]. Available: https://linkinghub.elsevier.com/retrieve/pii/S1050641119302536 (visited on 21/01/2021).

[17] M. Barbero, R. Merletti and A. Rainoldi, *Atlas of Muscle Innervation Zones*. Milano, Italy: Springer Milan, 2012, ISBN: 978-88-470-2463-2. DOI: 10.1007/978-88-470-2463-2. [Online]. Available: http://link.springer.com/10.1007/978-88-470-2463-2 (visited on 03/02/2021).

[18] R. Laurent, "Disorders of Skeletal Muscle," in *The Musculoskeletal System*, P. Sambrook, L. Schrieber, T. Taylor and M. A. Ellis, Eds., 2nd ed., Amsterdam, Netherlands: Elsevier, 2010, pp. 109–122, ISBN: 978-0-7020-3377-3. DOI: 10.1016/B978-0-7020-3377-3.00008-1. [Online]. Available: https://linkinghub.elsevier.com/retrieve/pii/B9780702033773000081 (visited on 03/02/2021).

[19] R. Merletti, A. Holobar and D. Farina, "Mathematical Techniques for Noninvasive Muscle Signal Analysis and Interpretation," in *Encyclopedia of Biomedical Engineering*, Amsterdam, Netherlands: Elsevier, 2019, pp. 95–111, ISBN: 978-0-12-805144-3. DOI: 10.1016/B978-0-12-801238-3.99987-2. [Online]. Available: https://linkinghub.elsevier.com/retrieve/pii/B9780128012383999872 (visited on 03/02/2021).

[20] R. Merletti and G. Cerone, "Tutorial. Surface EMG detection, conditioning and pre-processing: Best practices," *Journal of Electromyography and Kinesiology*, vol. 54, p. 102 440, Oct. 2020, ISSN: 10506411. DOI: 10.1016/j.jelekin.2020.102440. [Online]. Available: https://linkinghub.elsevier.com/retrieve/pii/S1050641120300821 (visited on 21/01/2021).

[21] H. J. Hermens, B. Freriks, C. Disselhorst-Klug and G. Rau, "Development of recommendations for SEMG sensors and sensor placement procedures," *Journal of Electromyography and Kinesiology*, vol. 10, no. 5, pp. 361–374, Oct. 2000, ISSN: 10506411. DOI: 10.1016/S1050-6411(00)00027-4. [Online]. Available: https://linkinghub.elsevier.com/retrieve/pii/S1050641100000274 (visited on 26/01/2021).

[22] SENIAM, *"SENIAM Recommendations"*, 1999. [Online]. Available: https://www.seniam.org/ (visited on 11/05/2021).

[23] R. Merletti, A. Botter and U. Barone, "Detection and Conditioning of surface EMG signals," in *Surface electromyography: physiology, engineering and applications*, R. Merletti and D. Farina, Eds., Hoboken, NJ, USA: Wiley, 2016, pp. 54–90, ISBN: 978-1-118-98702-5.

[24] B. Afsharipour, S. Soedirdjo and R. Merletti, "Two-dimensional surface EMG: The effects of electrode size, interelectrode distance and image truncation," *Biomedical Signal Processing and Control*, vol. 49, pp. 298–307, Mar. 2019, ISSN: 17468094. DOI: 10.1016/j.bspc.2018.12.001. [Online]. Available: https://linkinghub.elsevier.com/retrieve/pii/S1746809418303008 (visited on 04/02/2021).

[25] J. Rodriguez-Falces, D. Neyroud and N. Place, "Influence of inter-electrode distance, contraction type, and muscle on the relationship between the sEMG power spectrum and contraction force," *European Journal of Applied Physiology*, vol. 115, no. 3, pp. 627–638, Mar. 2015, ISSN: 1439-6319, 1439-6327. DOI: 10.1007/s00421-014-3041-4. [Online]. Available: http://link.springer.com/10.1007/s00421-014-3041-4 (visited on 05/02/2021).

[26] T. M. Vieira, A. Botter, S. Muceli and D. Farina, "Specificity of surface EMG recordings for gastrocnemius during upright standing," *Scientific Reports*, vol. 7, p. 13 300, Dec. 2017, ISSN: 2045-2322. DOI: 10.1038/s41598-017-13369-1. [Online]. Available: http://www.nature.com/articles/s41598-017-13369-1 (visited on 05/02/2021).

[27] J. K. Ng, V. Kippers and C. A. Richardson, "Muscle fibre orientation of abdominal muscles and suggested surface EMG electrode positions," *Electromyography and Clinical Neurophysiology*, vol. 38, no. 1, pp. 51–58, Feb. 1998, ISSN: 0301-150X.

[28] G. Boccia and A. Rainoldi, "Innervation zones location and optimal electrodes position of obliquus internus and obliquus externus abdominis muscles," *Journal of Electromyography and Kinesiology*, vol. 24, no. 1, pp. 25–30, Feb. 2014, ISSN: 10506411. DOI: 10.1016/j.jelekin.2013.10.017. [Online]. Available: https://linkinghub.elsevier.com/retrieve/pii/S1050641113002678 (visited on 26/01/2021).

[29] M. Beretta Piccoli, A. Rainoldi, C. Heitz, M. Wüthrich, G. Boccia, E. Tomasoni, C. Spirolazzi, M. Egloff and M. Barbero, "Innervation zone locations in 43 superficial muscles: Toward a standardization of electrode positioning: Innervation Zone Location and sEMG," *Muscle & Nerve*, vol. 49, no. 3, pp. 413–421, Mar. 2014, ISSN: 0148639X. DOI: 10.1002/mus.23934. [Online]. Available: http://doi.wiley.com/10.1002/mus.23934 (visited on 27/01/2021).

[30] A. Rainoldi, G. Melchiorri and I. Caruso, "A method for positioning electrodes during surface EMG recordings in lower limb muscles," *Journal of Neuroscience Methods*, vol. 134, no. 1, pp. 37–43, Mar. 2004, ISSN: 01650270. DOI: 10.1016/j.jneumeth.2003.10.014. [Online]. Available: https://linkinghub.elsevier.com/retrieve/pii/S0165027003003522 (visited on 03/02/2021).

[31] R. Merletti and H. Hermens, "Detection and conditioning of the surface emg signal," in *Electromyography: physiology, engineering, and noninvasive applications*, R. Merletti and P. Parker, Eds., Hoboken, NJ, USA: Wiley-Interscience, 2004, pp. 107–131, ISBN: 978-0-471-67580-8.

[32] J. Clark et al., *Medical instrumentation: application and design*, 4. ed, J. G. Webster, Ed. Hoboken, NJ: Wiley, 2010, OCLC: 552091465, ISBN: 978-0-471-67600-3.

[33] E. Peper, A. Booiman, I.-M. Lin, R. Harvey and J. Mitose, "Abdominal SEMG Feedback for Diaphragmatic Breathing: A Methodological Note," *Biofeedback*, vol. 44, no. 1, pp. 42–49, Mar. 2016, ISSN: 1081-5937, 2158-348X. DOI: 10.5298/1081-5937-44.1.03. [Online]. Available: https://meridian.allenpress.com/biofeedback/article/44/1/42/113592/Abdominal-SEMG-Feedback-for-Diaphragmatic (visited on 28/01/2021).

[34] A. Huebner, B. Faenger, P. Schenk, H.-C. Scholle and C. Anders, "Alteration of Surface EMG amplitude levels of five major trunk muscles by defined electrode location displacement," *Journal of Electromyography and Kinesiology*, vol. 25, no. 2, pp. 214–223, Apr. 2015, ISSN: 10506411. DOI: 10.1016/j.jelekin.2014.11.008. [Online]. Available: https://linkinghub.elsevier.com/retrieve/pii/S1050641114002454 (visited on 26/01/2021).

[35] D.-D. Ţarălungă, G.-M. Ungureanu, I. Gussi, R. Strungaru and W. Wolf, "Fetal ECG Extraction from Abdominal Signals: A Review on Suppression of Fundamental Power Line Interference Component and Its Harmonics," *Computational and Mathematical Methods in Medicine*, vol. 2014, pp. 1–15, Feb. 2014, ISSN: 1748-670X, 1748-6718. DOI: 10.1155/2014/239060. [Online]. Available: http://www.hindawi.com/journals/cmmm/2014/239060/ (visited on 07/05/2021).

[36] B. C. Fortune, A. Stewart, E. Hansenne, L. McKenzie, L. Chatfield and C. G. Pretty, "Design and testing of a low-cost electromyogram that uses a right leg driver circuit," in *2017 24th International Conference on Mechatronics and Machine Vision in Practice (M2VIP)*, Auckland: IEEE, Nov. 2017, pp. 1–6, ISBN: 978-1-5090-6546-2. DOI: 10.1109/M2VIP.2017.8211490. [Online]. Available: http://ieeexplore.ieee.org/document/8211490/ (visited on 19/02/2021).

[37] A. B. Romeo, C. Horellou and J. Bergh, "A wavelet add-on code for new-generation N-body simulations and data de-noising (JOFILUREN)," *Monthly Notices of the Royal Astronomical Society*, vol. 354, no. 4, pp. 1208–1222, Nov. 2004, ISSN: 0035-8711, 1365-2966. DOI: 10.1111/j.1365-2966.2004.08303.x. [Online]. Available: https://academic.oup.com/mnras/article-lookup/doi/10.1111/j.1365-2966.2004.08303.x (visited on 10/05/2021).

[38] M. Mohamed and M. Deriche, "An Approach for ECG Feature Extraction using Daubechies 4 (DB4) Wavelet," *International Journal of Computer Applications*, vol. 96, no. 12, Jun. 2014. DOI: 10.5120/16850-6712.

[39] P. Strumiłło and M. Rudnicki, "A Real-Time Adaptive Wavelet Transform-Based QRS Complex Detector, Adaptive and Natural Computing Algorithms," *Lecture notes in computer science*, vol. 4432, pp. 281–289, Apr. 2007. DOI: 10.13140/RG.2.1.1712.7847. [Online]. Available: http://rgdoi.net/10.13140/RG.2.1.1712.7847 (visited on 10/05/2021).

[40] G. Wang, Y. Zhang and J. Wang, "The Analysis of Surface EMG Signals with the Wavelet-Based Correlation Dimension Method," *Computational and Mathematical Methods in Medicine*, vol. 2014, pp. 1–9, Apr. 2014, ISSN: 1748-670X, 1748-6718. DOI: 10.1155/2014/284308. [Online]. Available: http://www.hindawi.com/journals/cmmm/2014/284308/ (visited on 10/05/2021).

[41] A. B. Romeo, C. Horellou and J. Bergh, "N-body simulations with two-orders-of-magnitude higher performance using wavelets," *Monthly Notices of the Royal Astronomical Society*, vol. 342, no. 2, pp. 337–344, Jun. 2003, ISSN: 0035-8711, 1365-2966. DOI: 10.1046/j.1365-8711.2003.06549.x. [Online].

Available: https://academic.oup.com/mnras/article-lookup/doi/10.1046/j.1365-8711.2003.06549.x (visited on 10/05/2021).

[42] G. Lu, J.-S. Brittain, P. Holland, J. Yianni, A. L. Green, J. F. Stein, T. Z. Aziz and S. Wang, "Removing ECG noise from surface EMG signals using adaptive filtering," *Neuroscience Letters*, vol. 462, no. 1, pp. 14–19, Oct. 2009, ISSN: 1872-7972. DOI: 10.1016/j.neulet.2009.06.063.

DEPARTMENT OF ELECTRICAL ENGINEERING
CHALMERS UNIVERSITY OF TECHNOLOGY
Gothenburg, Sweden
www.chalmers.se

CHALMERS
UNIVERSITY OF TECHNOLOGY